UNIVERSITY OF TWENTE.

BIOS
Lab on a Chip group

The entrapment and characterization of single spermatozoa in a microfluidic system

Jorien Berendsen

Report number: 2014-3
April 22, 2014

Committee:
Prof.dr.ir. A. van den Berg
Dr. L.I. Segerink
B. de Wagenaar, MSc
Dr.ir. N.R. Tas

Abstract

This research describes the entrapment of spermatozoa in a microfluidic device and the analysis of single spermatozoa by fluorescence and impedance spectroscopy.
This microfluidic device is made from PDMS and consists of two main channels, which are connected by small side channels. These side channels act as small traps when a pressure difference is obtained over the main channels. This pressure diffence was caused by a difference in flow rate. Three different trap heights of 1, 1.5 and 2 µm were tested, of which the 1 µm traps showed a single cell trapping capacity of 43%. This chip showed the least tendency to trap multiple spermatozoa, which is an advantage since multiple trapping is undesirable for impedance measurements.

Spermatozoa were analysed with fluorescent stainings. Viability staining was performed on and off chip. With viability staining on chip, the viability of a specific cell could be determined. FISH staining of X and Y chromosomes was performed, after which several FISH staining experiments were performed on spermatozoa on chip. The staining results were not influenced by the presence of microelectrodes in the chip.

The presence of a spermatozoon in the trap could also be detected through impedance spectroscopy. It was seen that spermatozoa caused a drop in impedance at the resistive plateau. This drop in impedance indicates that the interior of the cell was measured. Because the interior of spermatozoa mainly consists of DNA, it might be possible to measure the amount of DNA.

Therefore, viability and FISH staining on chip can be combined with impedance measurements on chip, to investigate the impedance differences of viable and dead spermatozoa and of X and Y bearing spermatozoa.

Contents

Chapter 1

Introduction

1.1 Project background

In the livestock industry, artificial insemination is a well-established method for expanding herds. Naturally speaking, the ratio of male to female offspring is around 50%. However, for some animal industries one specific sex is desired, e.g. female offspring for the milk and the pig industry. Performing artificial insemination with sex-sorted semen can provide a big economic benefit compared to insemination with normal semen.

This work is part of ongoing research to develop a microfluidic system, which is able to electrically detect whether a spermatozoon contains an X or Y chromosome and to subsequently sort them into two fractions. Currently, the most reliable method of sorting is fluorescence-activated cell sorting (FACS), a specialized flow cytometry sorting. A microfluidic system could provide two potential advantages: an increase in sorting efficiency and a decrease in inflicted cell damage.

1.2 Assignment description

This project focuses on fluorescent in situ hybridization (FISH) staining of the X and Y chromosomes of hydronamically trapped spermatozoa, which will serve as a verification tool for electrical measurements. The main goal is to perform FISH staining on trapped spermatozoa inside a microchannel. Firstly, viability staining will be performed in batch, and secondly in a microchannel. Subsequently, FISH staining will also be carried out in batch and in a microchannel. If FISH staining on chip is performed succesfully, electrical measurements will be integrated on chip.

1.3 Sex sorting background

At the moment, preselection of semen based on the sex chromosome is the most used in the animal livestock industry. In the beef industry, male offspring is preferred. Steers (castrated bulls) provide the most meat, so sperm sexing is used to select for males. In the dairy industry, only female offspring is desired for milk production. To ensure a genetic optimum, male calves are obtained from the best cows in the herd to use as breeding bulls.[1]

In the pig industry, female offspring is preferred, because they are necessary to maintain a healthy breeding stock and do not suffer from boar taint. Boar taint originates from male sex hormones that are absorbed into the fat. These hormones result in an unpleasant odor, which is present in

5% of uncastrated male pigs. due to this odor, the meat is preferably not used for consumption.[2]

1.4 Ethical concerns

When it is possible to do sex sorting in the veterinary industry, the same methods can be used for human spermatozoa. At the moment, sex selection on humans is only done in the case of heriditary diseases which are linked to the sex chromosomes. IVF is used, where the embryos are tested and selected on their sex chromosomes. Sex sorting before conception is also used, but current methods are less reliable and seen as too risky in the case of severe hereditary diseases. Also, this way of sorting damages the DNA. Reliable preconception sex sorting can make it easier to perform gender selection on humans without the need for a medical reason. This form selection might prevent the discarding of embryos of the wrong gender or cases of gender driven abortion. At the moment this is possible, as the gender can be discovered at the 20-week-ultrasound and in some countries (including the Netherlands) getting an abortion without giving any reasons is legal up to 24 weeks into the pergnancy.[3] There are however some concerns about the ethics of gender selection without a medical reason.

One concern is the potential of gender selection to increase or reinforce gender discrimination, either by allowing more males to be born as first children or by encouraging parents to prefer a gender.
A second concern is the welfare of children born as a result of gender selection, who may be expected to act in a gender specific way when the technique succeeds. The born children may also disappoint parents when they are born the "wrong" gender, as sex sorting is not (yet) 100% accurate.
The third concern is more of a societal concern. When widely practiced, gender selection could lead to imbalances in the sex ratio, as is already the case in some parts of China because of a one-child family policy. Another societal concern is the emphasis that gender selection could place on a child's genetic characteristics, rather than their inherent worth.
Before allowing the general public access to gender selection, a careful debate on the ethics of gender selection before conception is neccesary. [4]

1.5 Structure of the report

In chapter 2, the theory of this work is covered. Chapter 3 describes the materials and methods used for the experimental work. The results of the experiments are shown and discussed in chapter 4. Chapter 5 contains the conclusions and recommendations for further research.

Chapter 2

Theory

2.1 Sex determination

Most species on earth reproduce sexually, which means that for the formation of a new organism, a male and a female reproductive cell/gamete is necessary. These cells are formed from somatic cells in the body through meiosis. The male gamete is called a spermatozoon. A gamete is haploid, which means that only one of each chromosome is present in the nucleus. The fusion of two gametes produces an omnipotent stem cell, also called zygote. This zygote is diploid and has a pair of each chromosome, like normal cells in the body.[5] A human spermatozoon has 22 autosomal chromosomes and one sex chromosome. Bovine and porcine spermatozoa have 29 and 15 autosomal chromosomes respectively, with both containing one sex chromosome.[6]

In most mammals, the presence of a Y chromosome determines the sex of the offspring, as can be seen in Figure 2.1. This is the case even if there are more (or less) than 2 sex chromosomes through a mistake in the meiosis. This is possible through X inactivation (only one X chromosome is left activated, the rest is silenced) and the fact that the Y chromosome is gene poor (78 genes vs. about 2000 genes for the X chromosome). This means that for example individuals with 47,XXY and 47,XYY karyotypes are males, while individuals with 45,X and 47,XXX karyotypes are females. On the Y chromosome there is one gene, the sex-determining region of the Y, or SRY, that is the regulator of sex determination. This gene is located on the short arm of the chromosome.[5]

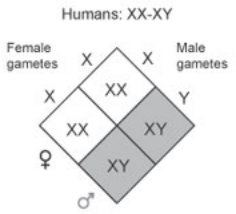

Figure 2.1: The presence of the Y chromosome determines the sex of the offspring. The female gamete delivers only X chromosomes, whereas the male gamete can have an X or a Y chromosome. Therefore, the sex chromosome content of the spermatozoon is decisive for the sex of the offspring.[5]

2.2 Anatomy of the spermatozoon

Spermatozoa have evolved to most efficiently fertilize an egg cell, or ovum. They are equipped with a strong tail, which propels them through an aqueous medium. Compared to other cells present within the body, the only organelle present in the sperm cell is the mitochondrium. Other cell organelles are unnecessary for the task of delivering the DNA to the ovum.[7]

Spermatozoa usually consist of three regions enveloped by a plasma membrane: the tail, the midpiece and the head (Figure 2.2). The DNA inside the head is very condensed, which minimizes the cells volume to have a faster transport. In the front of the head, the acrosomal vesicle is located. This vesicle contains enzymes that help the sperm to penetrate an ovum's outer coat.[7] The tail of a sperm is a long flagellum. The flagellar movement of the tail is driven by motor proteins, which use the energy created by ATP hydrolysis. The mitochondria are located in the midpiece and produce the ATP to power the flagellum.[7] Typical dimensions of a spermatozoon of different species are given in Table 2.1

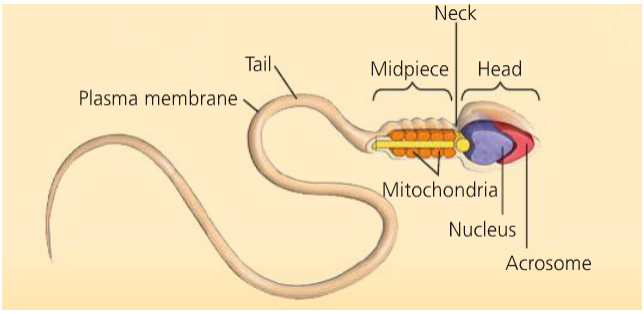

Figure 2.2: A spermatozoon consists of three distinct regions; the head, the midpiece and the tail. The head contains a nucleus and an acrosome and the midpiece contains mitochondria.[7]

Table 2.1: The dimensions of human, porcine and bovine spermatozoa.

	Total	Head		Midpiece		Tail	
Species	Length	Length	Width	Length	Width	Length	Width
Human [8]	55 µm	4.5 µm	3 µm	4.2 µm	0.6 µm	45 µm	0.5 µm
Domestic Pig [9]	45 µm	7 µm	4 µm	9 µm	0.7 µm	28 µm	0.4 µm
Cattle [10]	57 µm	7 µm	4 µm	10 µm	0.6 µm	37 µm	0.4 µm

2.3 DNA

DNA is composed of four different nucleobases, sugars and phosphates. Adenine (A) and Thymine (T) each form two hydrogen bonds and Guanine (G) and Cytosine (C) form three hydrogen bonds. Thermodynamics dictate that the only pairs that will exist will be A-T and G-C, because formed hydrogen bonds are energetically very favorable (Figure 2.3a).

Because the phosphate and the sugar of the nucleotides are situated not exactly above each other, they will form a double helix when they are stacked. This helix will have two different grooves, as the two backbones, consisting of the sugars and phosphates, are not exactly opposite of each other (see Figure 2.3b). These grooves can serve as binding sites for different proteins and fluorescent

dyes (such as DAPI, see Appendix B.2). DNA is normally also methylated, where a methyl group is added to the cytosine or adenine nucleotides.[11]

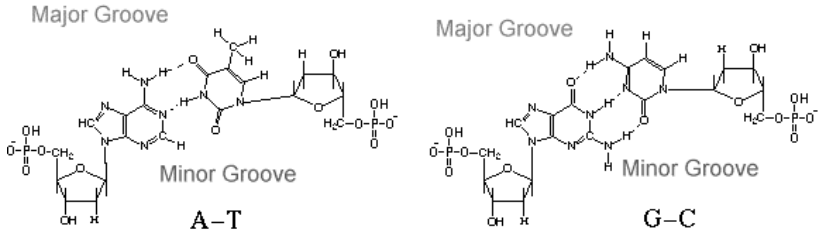

(a) DNA base pairs

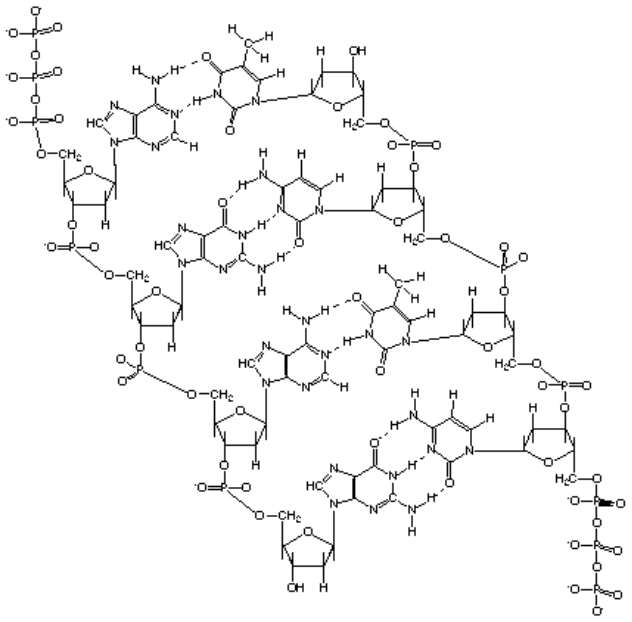

(b) DNA Stacking

Figure 2.3: DNA is composed of four nucleotides, where the bases A and T and the bases G and C form hydrogen bonds. The placing and structure of the sugars and phosphates, that are connected to the bases, give rise to two different grooves and a double helix structure.[11]

To achieve a tight packing in the nucleus, the DNA is coiled around nucleosomes, which are complexes of positively-charged histones (proteins) that strongly bind to the negatively-charged phosphate-spine of the DNA helix. These nucleosomes, together with histones, help the DNA to fold up into a chromosome. This process is illustrated in Figure 2.4.[12]

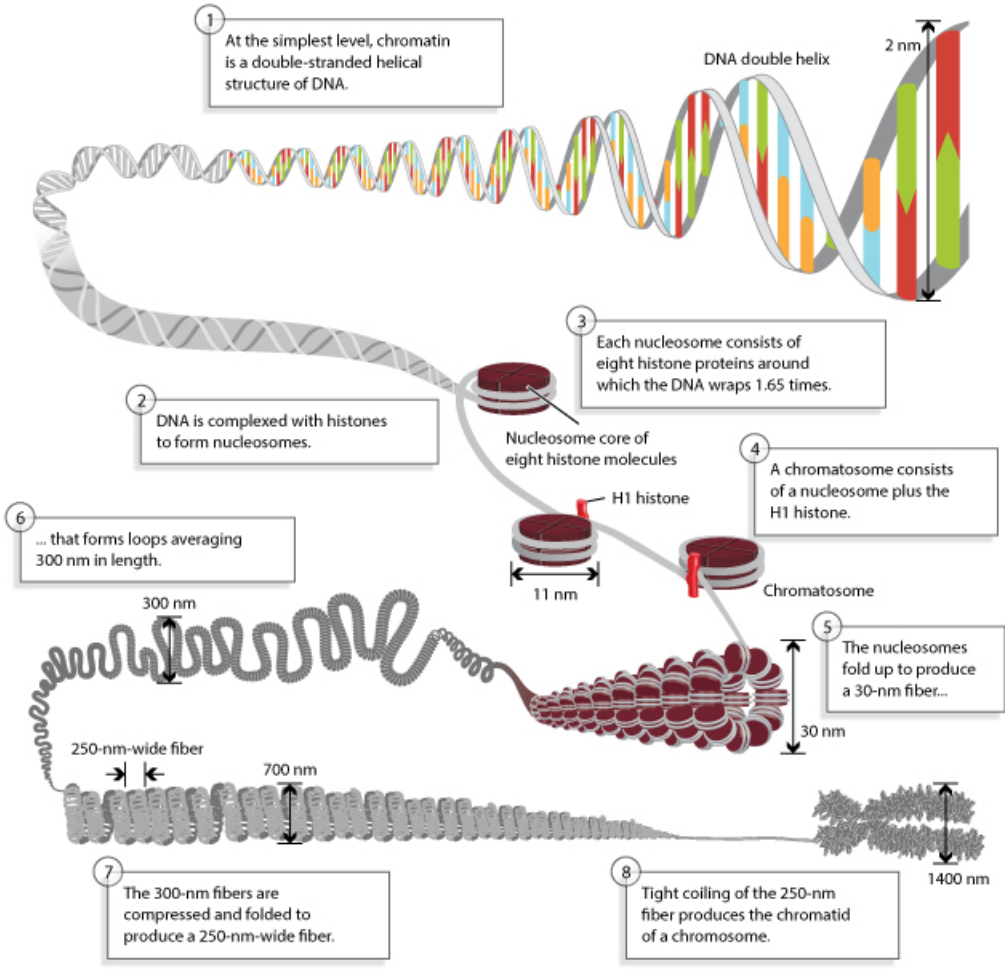

Figure 2.4: The DNA condensation process from double helix to chromosome.[12]

Inside the nucleus of a spermatozoon, the DNA is packed even tighter. To achieve this, approximately 85% of the histones are replaced by protamines. These protamine complexes do not coil around each other like the nucleosomes, but form thoroids that stack above each other (see Figure 2.5). Besides DNA, also trace amounts of proteins and nonencoding RNA can be found inside the nucleus.[13]

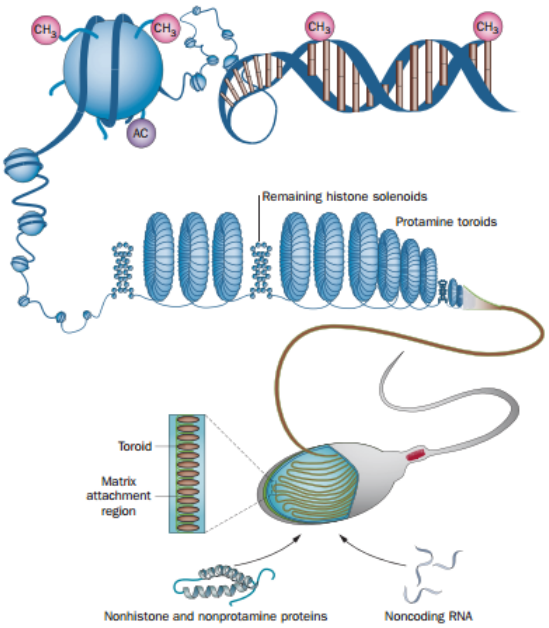

Figure 2.5: The DNA condensation process in spermatozoa, where most of the histones are replaced by protamines, causing a tighter packing than in somatic cells.[13]

2.4 Fluorescent staining

Fluorescence is the emission of photons due to the relaxation of photon exited electrons. The energy difference between the energy states determines the wavelength of the emitted light. On average, this emitted light will be lower in energy than the light absorbed by the molecule, due to vibrational relaxation (both after absorption and after emission). The change in photon energy causes a shift of the fluorescence spectrum to longer wavelengths than the absorption spectrum. This phenomenon is known as the Stokes Shift.[14] Figure 2.6 shows the mechanism of fluorescence.

Fluorescence microscopy is the most common technique to visualize biological structures and processes. The goal in fluorescence microscopy is to choose an appropriate excitation wavelength to excite the dye molecule. Using a white-light-source, a band-pass filter (excitation filter) is selected, which transmits only a small bandwidth of wavelengths suitable for the fluorophore. Exciting a dye molecule at a nonoptimal wavelength will decrease the amount of emitted fluorescence light, but not the characteristics of the emission spectrum.[15]

Cells do not react favorably to photons with a large energy (light in the UV spectrum). Compounds that absorb in the visible region of the spectrum generally have some weakly bound or delocalized electrons. Most fluorophores thus consist of conjugated systems.[16] In Table 2.2 an overview of some fluorophores is seen, which are used for fluorescent staining of cells.

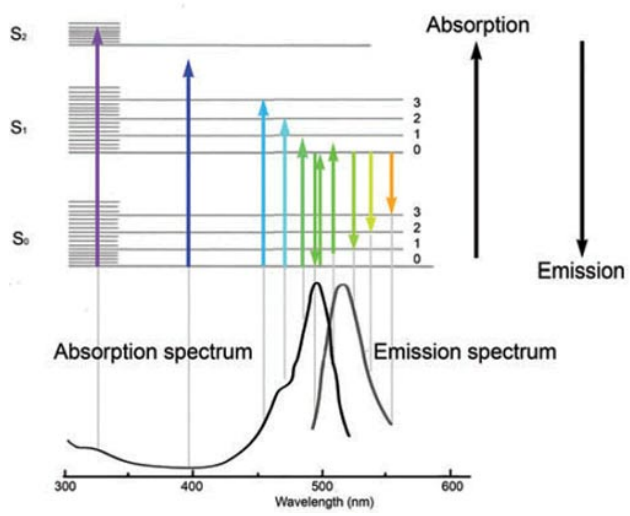

Figure 2.6: Jablonski diagram, which shows the mechanism of fluorescence.[17]

Table 2.2: Excitation and emission maxima for the used dyes in this work. For more information on the dyes, see Appendix B.

Dye	Excitation max (nm)	Emission max (nm)
SYBR 14	488	516
Propidium Iodide	536	617
IDetect Red	548	573
IDetect Green	493	521
DAPI	360	460

2.4.1 Viability staining

Viability staining is used to determine if a cell is dead or alive. This can be done by staining the cells with two fluorescent dyes. These dyes bind to the DNA helix. The dyes are chosen such that one of the dyes will be able to permeate the cell membrane and color the DNA of all cells. The other dye is not able to go through an uncompromised cell membrane and will only color the dead cells. In this work, the dyes SYBR 14 and propidium iodide (PI) are used. SYBR 14 is able to permeate the cell membrane and color all cells. PI can only stain the DNA of cells with compromised cell membranes, which are dead cells, as it is a nonpervasive dye. Because the binding to DNA is more favourable for PI, this dye expels the SYBR 14 from dead cells. Possible binding sites for fluorescent dyes used in viability staining are shown in Figure 2.7. SYBR 14 and PI are both intercalators.[18]

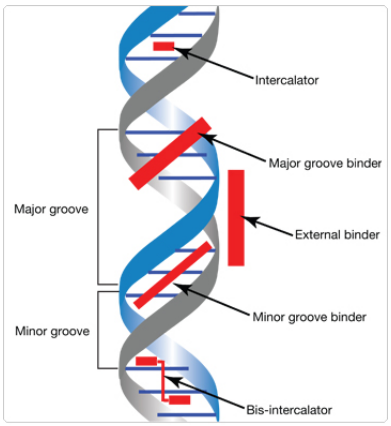

Figure 2.7: There are several binding sites on the DNA. The two largest classes of dyes are intercalators and minor groove binders.[18]

2.4.2 FISH staining

FISH staining is used to detect specific genes/sequences on the DNA of a cell. To detect such a specific DNA sequence, fluorescent probes can be used. These probes consist of a strand of complementary DNA, whose nucleotides bind to the chromosomal DNA that has to be detected. This mechanism for detection is called Fluorescence In Situ Hybridization, or FISH.

Because of the hydrogen bonds between the bases, a DNA helix is remarkably stable. When breaking down the hydrogen bonds of the helix with heat or chemicals, the helix is able to reform when conditions become more favorable. This ability of the DNA helix to reform, or renature, provides the basis for molecular hybridization.

The first step in the FISH process is to make a copy of the chromosomal DNA sequence that is of interest, and label this strand directy or indirectly by a fluorescent marker (Figure 2.8b, middle or left column). This copy serves a the fluorescent probe and will be bound to the target DNA. Because DNA inside a spermatozoon is tightly packed, it must first be decondensed. This step is necessary for the accessibility of hybridization sites. Next, both the target and the probe sequences must be denatured, which is done by exposing the DNA to heat or chemicals (Figure 2.8c). This denaturation step is necessary to break down the hydrogen bonds. The sequences are then mixed (Figure 2.8d) and during the hybridization step, the probe will hybridize to its complementary sequence on the chromosome. The DNA is renatured in the double helix after the hybridization, with the labeled probes on the specific target sequences. If the probe is already fluorescent (middle column), the site of hybridization can be directly detected, otherwise an additional step is necessary. The hybrids formed between the probes and their targets can be detected with the usage of a fluorescent microscope.[19] The more technical processing steps can be found in the protocols in Appendix A.2.

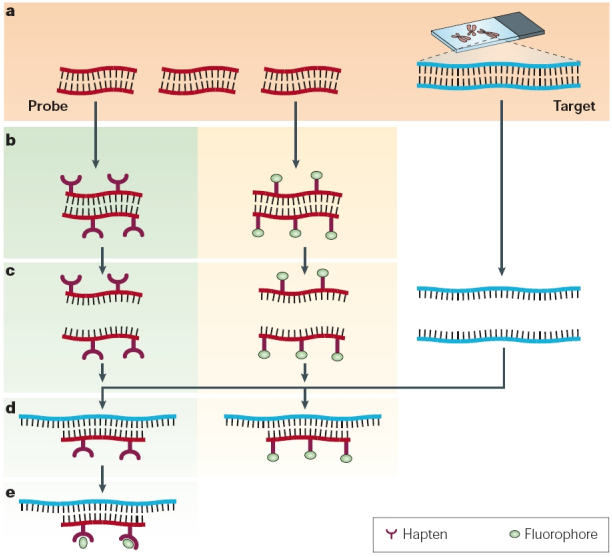

Figure 2.8: Before hybridization, the DNA probe is labeled. Two labeling strategies are commonly used: indirect labeling (left) and direct labeling (right). For indirect labeling, probes contain an antigen, while with direct labeling the probes contain a fluorophore. The labeled probe and the target DNA are denatured, followed by the (re)annealing of complementary DNA sequences, inserting the probe in the DNA. In case of indirect labeling, an extra step is necessary to make the probe fluorescent. The sample is then ready for visualization.[19]

Various probes can be used for FISH staining, with each their own application. In this work, locus specific probes are used. This probe is very useful if the research needs information on a specific chromosome sequence. A chromosome with a locus specific probe is visible in Figure 2.9.[19]

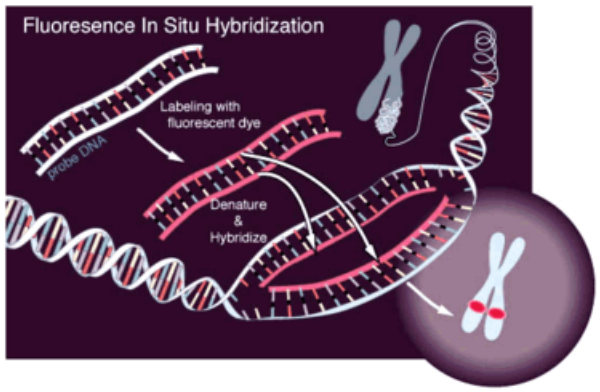

Figure 2.9: The locus specific probe binds to its target sequence, showing two fluorescent spots on the chromosome.[20]

2.5 Current methods for sex sorting

The two currently used techniques for sex sorting of semen are centrifugation and FACS. These techniques are based on the fact that an X spermatozoon has 3.8% more DNA than a Y spermatozoon, resulting in a difference in sperm mass.[21]

2.5.1 Centrifugation

When a semen sample is centrifuged, the induced forces cause the spermatozoa (and other particles) in the sample to become sorted into layers according to their density. Sorting separates the more dense X spermatozoa from the lighter Y spermatozoa. By separating the layers, sperm populations with a skewed ratio of X to Y chromosome content can be obtained.[22]

The accuracy of this method is influenced by confounders such as the natural spreading of the spermatozoa size in every individual and between individuals. The threshold for the best separation is thus different for every sorting.[23] This method has been tested and has both been reported as succesful, with an enrichment of aproximately 70%,[24] and unsuccesful to alter the X/Y ratio in sperm enough for clinical use.[25]

2.5.2 Fluorescence Activated Cell Sorting (FACS)

FACS is a specialized type of flow cytometry. Flow cytometry can be used to count and sort cells. This is done by suspending the cells in fluidstream and passing them through a detection apparatus. FACS is based upon the specific light scattering and fluorescent characteristics of each cell. When sex-sorting spermatozoa, the DNA is stained with the fluorescent dye Hoechst 33342. As a spermatozoon with an X chromosome has more DNA than a spermatozoon carrying a Y chromosome, a difference in fluorescence can be detected. The spermatozoa are then passed through a cell sorter (of which a schematic representation is visible in Figure 2.10), where they are divided in three

groups; X bearing spermatozoa, Y bearing spermatozoa and a waste category. The advantage of it is the increased accuracy, with a purity of the sexed samples of 80% and up to more than 90%. The disadvantages of this technique compared to the centrifugation are the higher costs and the induced damage to the sperm cells.[26]

FACS is the most used method for sex sorting. Spermatozoa can be sexed at a rate of 3000 live spermatozoa per second. The theoretical maximum rate is estimated to be at 10,000 spermatozoa per second. About a quarter of the spermatozoa processed are efficiently sex-sorted; the rest is discarded in the process or lost due to logistical constraints. The fertility is somewhat lower with sexed than control spermatozoa.[27]

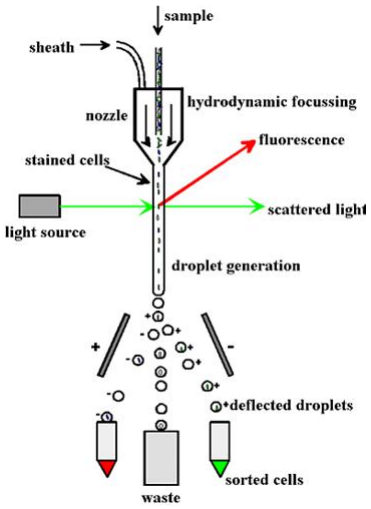

Figure 2.10: Before going into the cell sorter, the DNA of the cells in the semen sample is stained with a fluorescent dye. The sample is forced out of a nozzle in a small stream. When the stream of cell containing fluid is passed through a UV laser beam, the fluorescent stained DNA starts to emit. The intensity of the fluorescence is measured. The stream is then broken into micro-droplets that optimally hold one spermatozoon. If the measured amount of fluorescence is in the range designated for the Y spermatozoa, that micro-drop is given an electric charge by passing through a charged ring. If the intensity is within the range for X spermatozoa, the micro-drop is given an opposite electric charge. The charged micro-drops fall between two charged plates, resulting in two groups of droplets to be separated into different pools. Droplets that fall outside of the fluorescence range for X or Y, for example when there are two spermatozoa in one droplet, are collected into a third group.[28]

2.6 Cell trapping techniques

There are several techniques available to trap cells within microfluidic systems. Well described methods include hydrodynamical trapping and electrical trapping, which by electrophoresis and the use of an optical tweezer. Lastly there are some other methods, such as acoustic and magnetic trapping.

2.6.1 Hydrodynamical trapping

The most straight forward way to realize cell or particle trapping in microfluidic systems is to use hydrodynamics. This can be done by creating obstacles for the cells (see Figure 2.11) or by creating side channels in a main transport channel. In the second method, the side channel dimensions are

sufficiently small to trap cells when a fraction of the total flow is sucked through these channels by a pressure difference (see Figure 2.12).[29, 30, 31] This method has been used to trap different cells, but not yet for spermatozoa.

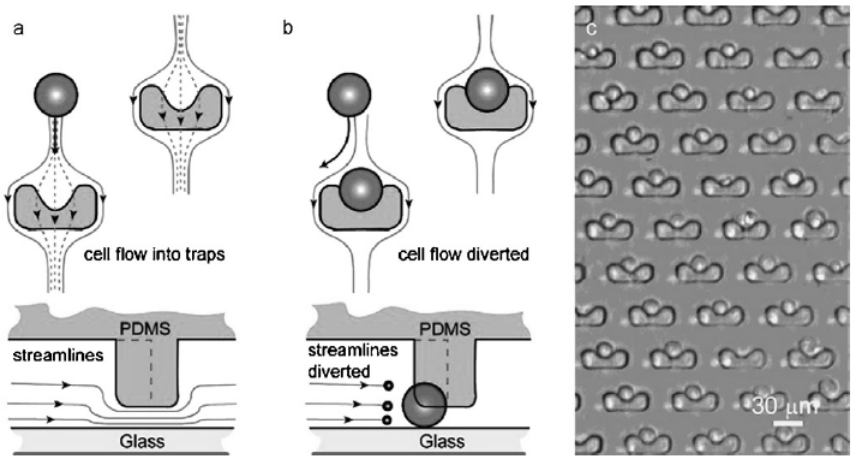

Figure 2.11: For this particular set-up, two-layer (40 and 2 µm) cup-shaped PDMS trapping sites allow a fraction of the fluid streamlines to enter the traps. After a cell is trapped and partially blocks the 2 µm open region, the amount of streamlines through the trap decreases, discouraging other cells to enter the traps and leading to single-cell trappings.[30]

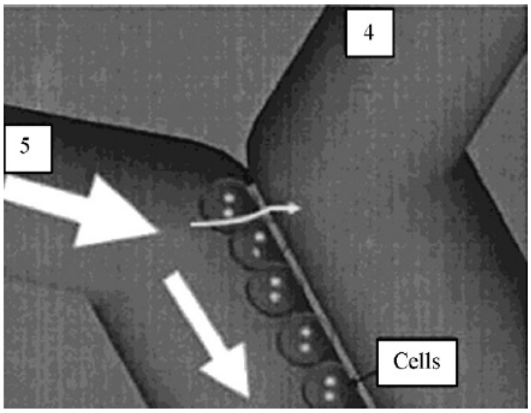

Figure 2.12: When the liquid pressure in channel 5 is higher than in channel 4, a fraction of the fluid flows over the dam structure to channel 4. The hydrodynamic pressure difference will cause the cells in channel 5 to be trapped at the trapping channels of the dam. After the cells are trapped, they (partially) block the flow, diverting other cells and leading to single-cell trapping.[31]

2.6.2 Electrical trapping

Electric fields can be used to trap spermatozoa in several ways. With dielectrophoresis, a force is exerted on a particle due to an inhomogeneous electric field. This forced is caused by the polarization of the particle, which is then moved across the field gradient. Fuhr et al. demonstrated the use of two methods which make use of negative dielectrophoresis. A quadrupole/octopole cage and strip wise arranged electrodes can be used to generate these fields. The typical field distributions of such systems can be seen in Figure 2.13.[32]

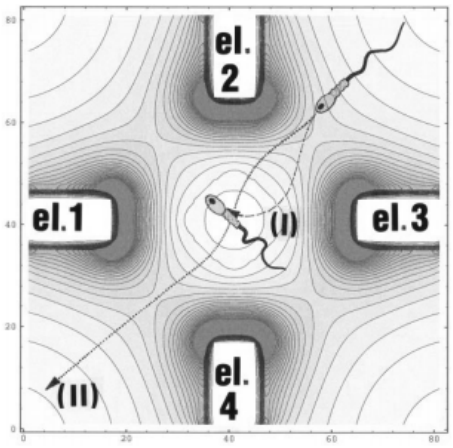

(a) There is a higher conductivity around the spermatozoa at larger frequencies (in the MHz range). Because of this, negative dielectrophoresis can be used to focus the spermatozoa towards a lower electric field strength. The electrodes are focused in such a way that the field minumin is located in the center of the trap. Only slowly moving spermatozoa can be forced to a stop (I). Faster swimming spermatozoa can only be deflected (II), as the forces involved are not that large.[32]

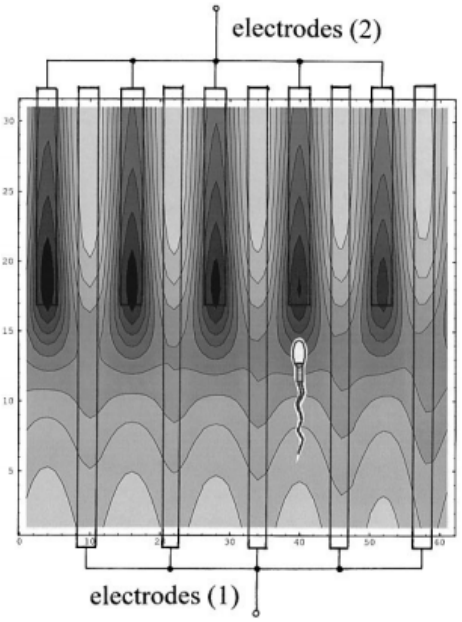

(b) This method makes use of electrodes and a hydrodynamical flow. Depending on its motility, a spermatozoon finds a stable position in front of the break-electrodes (2). This is the equilibrium point between the sperm forces, the repelling electric field force and the hydrodynamic force. Rapidly swimming spermatozoa stop close to the break-electrode, whereas slower swimming cells come to rest further away.[32]

Figure 2.13: Spermatozoa can be captured by different dielectrophoretic methods. The field distributions of a quadrupole/octopole cage (a) and stripwise arranged electrodes (b) are visible. Darker colors indicate larger fieldstrengths.[32]

The optical tweezer technique uses the electromagnetic fields of light. Here, a force is generated by a single beam gradient laser to trap a spermatozoon. If the particle is pulled sideways from the focus center, the trap beam will pass through the edge of the particle. Just like with a lens, the rays will be refracted towards the optical axis. If the particle moves up, it focuses the outgoing beam into a narrower bundle. There are then sideways and upward forces on the laser beam, caused by the direction and thus momentum change of the electromagnetic field. Such a force results in an opposite force on the particle. This keeps the particle at the center of the trap, where the light rays will pass through symmetrically.[33] With this technique spermatozoa can also be trapped, as shown in the work of Nascimento et al.[34]

2.6.3 Other trapping techniques

Accoustic trapping is also possible. A standing ultrasonic wave generates stationary pressure gradients. In a liquid medium, these pressure gradients exert forces on particles that differ in density and compressibility from the medium. The particles are then directed to the pressure nodes of the standing wave.[29] Another technique uses microcontact painting. With this technique, protein spots are patterned on a substrate. Frimat et al. showed that they are able to trap and optically analyse single spermatozoa using this technique.[35]

Magnetic trapping techniques make use of magnetic fields and magnetic particles of different kinds and sizes. Magnetic methods can also be used to trap non-magnetic objects if a suitable magnetic buffer is chosen. In a homogeneous field, where there is no magnetic gradient, there isno force acting on a particle. It is thus necessary to create an inhomogeneous magnetic field to manipulate a particle. The set-up to create such a field is generally called a magnetic tweezer. The force on a particle that can be generated by this method is typically between a few pN to tens of pN.[36]

2.7 FISH staining on chip

In the following examples, FISH has been performed on chip to reduce time steps and the amount of reagents, especially the amount of expensive probes. Although it is shown for different cells on chip, FISH staining on chip has not been performed on spermatozoa.

In the first example, Matsunaga et al. made a microfluidic device (shown in Figure 2.14) with a black PET micromesh for the entrapment of cells. Cell adsorption on other sites was prevented by treating the PDMS surface of the microchannel with air plasma and Pluronic F-127. The FISH staining could then be directly performed against cells that have been trapped onto the black PET micromesh.[37]

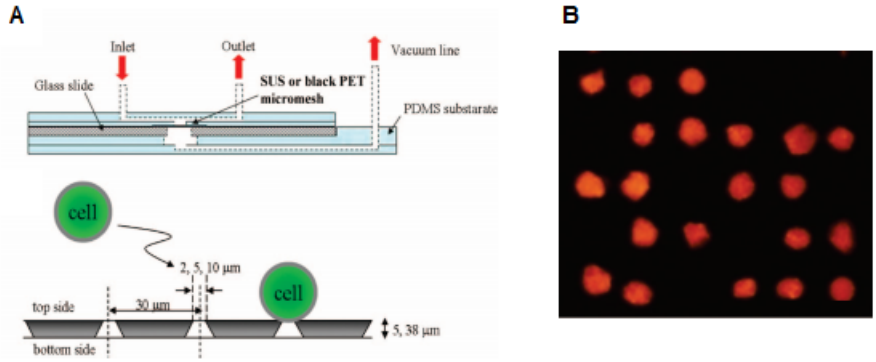

Figure 2.14: A: A schematic diagram of the PDMS microfluidic device integrated with a micromesh for entrapment of mammalian cells. Top; the PDMS microfluidic device integrated with micromesh for entrapment of mammalian cells. Bottom; the black PET micromesh. B: A fluorescence microphotograph of the FISH stained β-actin mRNA in Raji cells that were trapped on the black PET micromesh.[37]

A second example is an integrated and automated on-chip FISH implementation (shown in Figure 2.15), which requires only a few minutes of setup time. Sieben et al. claim that their device has lowered the reagent use by 20-fold, decreased the labour time by 10-fold, and substantially reduced the amount of support equipment needed. Also, a hybridization time of 1 hour was reported.[38]

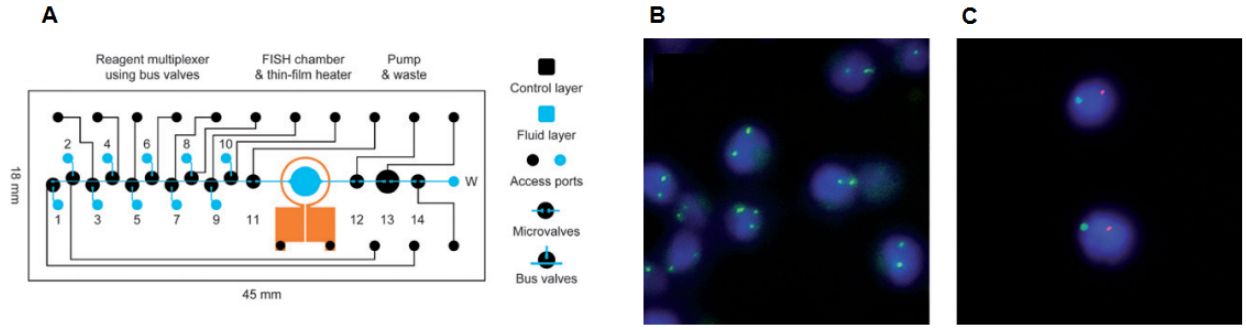

Figure 2.15: A: The microchip contains a reagent multiplexer, a cell chamber with an integrated thin-film heater and a pump. The reagent multiplexer was made of bus valves with minimal dead volume, to avoid the mixing of reagents. During the process, vacuum is constantly applied to the waste well (W). Next to the device, two fluorescence images are shown, which were made after the automated FISH protocol was performed on the integrated microchip. B: Two X chromosomes were detected, C: An X and Y chromosome were detected.[38]

A third example is a device (Figure 2.16) that is used for preparing metaphase spreads on a microscope glass slide, followed by a adhesive tape-based bonding protocol for the fabrication of the microFISH device. Vedarethinam et al. claim that the microFISH device allows for an optimized metaphase FISH protocol on a chip with a 20-fold reduction in the reagent volume, although the amount of the expensive probe was only halved.[39]

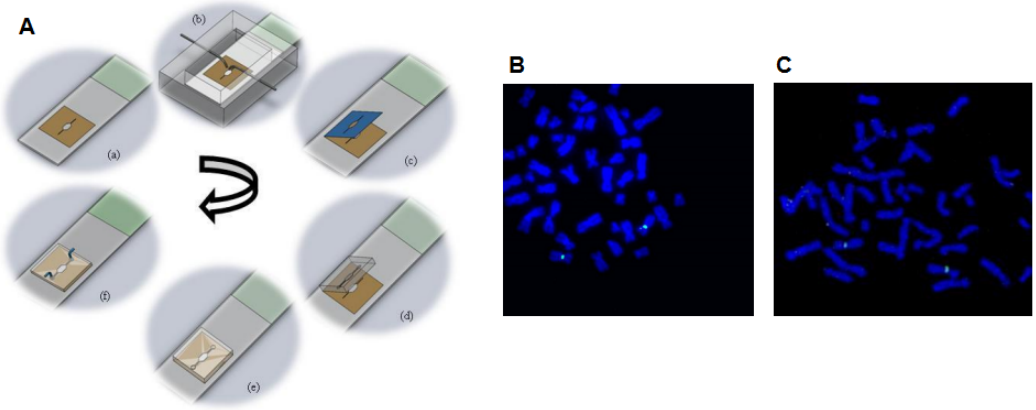

Figure 2.16: A: The pre-FISH process is visible. (a) Placing the double-sided adhesive tape stencil on the slide; (b) Spreading of the metaphase spreads in the splashing device; (c) Removing the top cover of the double-sided tap; (d)/(e) Aligning and placing the PDMS onto the tape; (f) Connecting the syringes. B: The fluorescence image of normal FISH staining. C: The results from the on-chip staining. A slight decrease in intensity is visible when the on-chip staining is compared with the normal staining process.[39]

2.8 Impedance spectroscopy

The response of a material to an applied electric field is described by its conductivity (σ, in S/m) and permittivity (ε,in F/m). The conductivity gives a measure of its ability to conduct an electric current, whereas the permittivity gives a measure of the ability to store charge when under the influence of an electric field. The conductivity and permittivity are related due to the fact that energy cannot dissapear, it has to be either stored or passed through.

The conductivity and permittivity are combined into the complex permittivity ε^*, where $\varepsilon^* = \varepsilon + \mathrm{j}\frac{\sigma(\omega)}{\omega}$. Here ω is the radial frequency ($\frac{\mathrm{rad}}{\mathrm{s}}$) and $\mathrm{j} = \sqrt{-1}$. The real part of this value is generally called the resistance, while the imaginary part is called the reactance. Together they form the electrical impedance. The electrical impedance is the measure of the opposition that is presented to an anternating current of a certain frequency. It is defined as $\frac{\mathrm{V}}{\mathrm{I}}$, where V and I are the complex voltage and current. The complex permittivity (or impedance) can be measured by dielectric spectroscopy (or impedance spectroscopy).[40]

2.8.1 Dielectric properties of cells

A cell consists of a cell membrane and the cytoplasm. The cell membrane is a lipid bilayer, while the cytoplasm is composed of the cytosol and organelles. The cell membrane generally has a small reactance and a large resistance. The reactance of the cytoplasm is very large when compared to its resistance. [41]

2.8.2 The equivalent circuit model

To gain insight in the electrical properties of a cell, an equivalent circuit model (ECM) can be constructed. There are three main linear components in such a circuit. There are capacitors, inductors and resistors, of which the impedances are given by $\frac{1}{\mathrm{j}\omega\mathrm{C}}$, $\mathrm{j}\omega\mathrm{L}$ and R respectively. As inductors do not appear in our ECM, these are not further discussed.
The phaseshift of a capacitor is -90°, while a resistor does not change the phase, because they do not store charge. The magnitude of the impedance of a capacitor will decrease as the frequency goes up, as it is inversely proportional to the frequency. At higher frequencies, the capacitor has less time to charge, until it becomes a short. The impedance of a resistor is independent of the frequency, and will thus stay the same over the complete frequency range.

In Foster and Schwan's simplified circuit model for a single cell, the following approximations are made. The lipid bilayer membrane can be approximated by a capacitor, as it has a large resistance, but a small reactance. Cells themselves are able to contain a voltage drop over the membrane, indicating the capacitive properties of the lipid bilayer. The cytoplasm can be modeled by a resistor, as its reactance can be ignored when compared to its resistance. The cytoplasm of a spermatozoon generally does not contain any significant bilayers, which are mainly responsible for any reactance in biological systems.[41] Figure 2.17 shows the simple ECM for a cell.

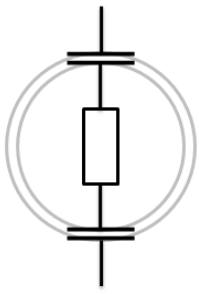

Figure 2.17: ECM for a cell according to Foster and Schwan's simplified model.

2.9 Previous projects

This work is a follow-up on the research done by two other students. The first student, Camille Denoeud, researched a way to trap spermatozoa in a microchip. The second student, Inge van de Ven, worked on (the protocol for) FISH staining of spermatozoa.

2.9.1 Results from project 1

This work focused on designing a microfluidic chip for the single cell entrapment of spermatozoa. For the entrapment of spermatozoa, five trapping techniques were considered: dielectrophoresic, optic, acoustic, magnetic and hydrodynamic entrapment. These trapping techniques are described shortly in section 2.6.

This dielectric trapping method was not suited due to the cost and complexity of the electrode microfabrication. Furthermore, it would complicate electrical measurements. The optical tweezer technique has a small trapping time and a large and expensive set-up, which makes it unattractive. Acoustic trapping can be accomplished with an easy set-up, but it has a tendency to form clusters, making it very hard to trap a single spermatozoon. With magnetic entrapment, it is almost impossible to provide enough force to trap a spermatozoon, as only forces tens of pN instead of 200 pN (the force generated by a spermatozoon) are achieved. Therefore, hydrodynamic entrapment was chosen, which fit all of the requirements in Table 2.3. It has an easy set-up, a long trapping time, and the integration of a large possible amount of traps.
Because spermatozoa are motile cells, the side channel trapping method was chosen. This method makes it harder for the cells to escape and easier to be caught than an obstacle method, as the tail is very large in comparison to the head (giving problems with smaller obstacles). Electrical measurements are also more easily carried out with a side channel set-up than an obstacle set-up, where the obstacles might influence the measurements.[42]

Table 2.3: Comparison of the different methods with the requirements.[42]

	Criteria				
Trapping method	Easy set-up	Trapping time t>40s	F>200pN	PDMS	Multiple traps
Dielectrophoretic	-	+	+	+	+
Optical	-	-	+	-	-
Acoustic	-	-	+	-	+
Magnetic	-	+	-	-	-
Hydrodynamic	+	+	+	+	+

The designed microchip for this project was fabricated from PDMS, because it is easy to use, cheap and biocompatible. The design has the following dimensions: the height of the trapping channel is 2 µm and that of the main channel is 20 µm. The width of the main channel is 100 µm, to allow the cells to flow undisturbed, and the width of the trapping channel is 2 µm. The length of the trapping channel is 20 µm. The chip design is shown in Figure 3.1. To prevent cells sticking to the PDMS walls, the semen was diluted in accutase. A low concentration of spermatozoa also gave a better and cleaner trapping yield. A concentration of $1 \cdot 10^6$ ml^{-1} was reported to give the best yield, with 55%.[42]

2.9.2 Results from project 2

The project was based on a reported FISH protocol for boar spermatozoa. Obtained results were used to optimize the protocol. Adjustments were made by varying the incubation times, the solutions for decondensation and the incubation temperature. The critical steps in the protocol were the DTT step and the washing step. The optimized FISH protocol (Appendix A.2) was used for the current project.[43]

Chapter 3

Experimental set-up

3.1 Chip fabrication

PDMS chips were used for this project. These chips contain two main channels, interconnected by 20 side channels. These side channels act as cell traps when there is a pressure difference between the main channels. Three PDMS chips were used, where the traps have channel heights of 1, 1.5 and 2 μm respectively. The PDMS chips were made from a mold, which is a reusable SU-8 (an epoxy based negative photoresist) patterned silicon wafer. In Figure 3.1 an overview of the chip design is shown.

In the fabrication of such a mold, negative photoresist layers were patterned on a 4-inch silicon wafer. First, the wafer was cleaned and a 30 nm aluminum layer was deposited by sputtering on the wafer. After this layer had been etched away, the alignment mark, that is included in all mask layers, was clearly visible for alignment. The molds used in this project contain two different layers of SU-8. The layers have heights of 1, 20 μm, 1.5, 20 μm and 2, 20 μm respectively. The other dimensions of the chip can be seen in Figure 3.1. Alignment was performed very precisely, because the margin is less than 1 μm. To prevent a bad coverage, the process was started with the thinnest layer. When exposed to UV light, the long molecular chains in SU-8 cross-link, causing the solidification of the material. After exposure through the mask, the unexposed part of the wafer was etched away. To strengthen the mold, a dummy wafer was glued on the backside.[42]

After the mold was ready, PDMS chips were by pouring PDMS on the mold and curing it at 60°C. The PDMS was made by mixing two components, the polymer base and the cross linker together in a ratio of 10:1. This mixture was first degassed, to remove air bubbles that where created during mixing. The PDMS was then poured on the mold, after which a second degassing took place. This second degassing ensured the removal of any possible air bubbles on the micro pattern. The PDMS was then cured overnight at 60°C for complete crosslink formation (for the complete protocol, see Appendix A.3).

After the PDMS was cured, it was peeled from the wafer. Holes were punctured in the chip with a hollow needle of the desired width to form in- and outlets. The punctured chips were then cut from the PDMS plate with a razorblade. The chips and glass slides (or glass chips with platinum electrodes) were then cleaned with SCOTCH tape. The surfaces of the PDMS and the bonding glass were treated with oxygen plasma in a plasma cleaner for 45 seconds at 400 mTorr. The treated PDMS was then placed onto the treated glass surface. The chip was pressed carefully to seal it

properly. Next, the slides were placed in an oven at 60°C for 30 minutes. This permanently seals the substrates together. The protocol for the PDMS chip fabrication can be found in Appendix A.3.

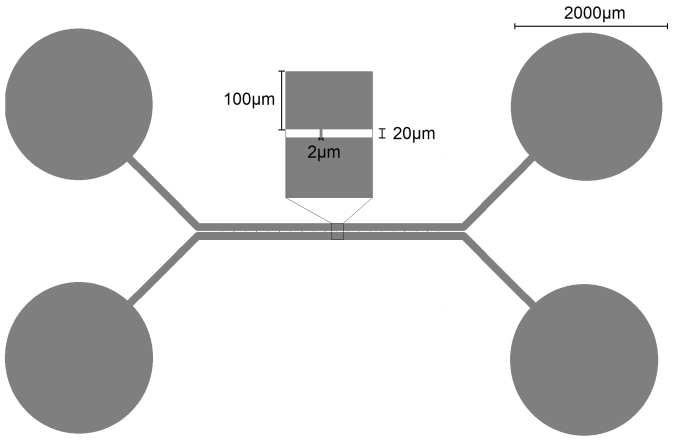

Figure 3.1: The PDMS chip.

3.2 Electrode design and set-up

For the impedance measurements, two planar electrode designs were fabricated. A planar set-up was chosen for its ease of fabrication. The electrodes in design 1 have a width of 20 µm with an overlap of 25 µm. The electrodes in design 2 were made with three different widths; 10, 20 and 40µm. The electrodes are present on a glass chip, which is embedded in a custom-made printed circuit board (PCB) (see Figure 3.3). The alignment of the chip on the micro electrodes was done with a special alignment tool under a stereomicroscope (Appendix C). The two design are show in Figure 3.2.

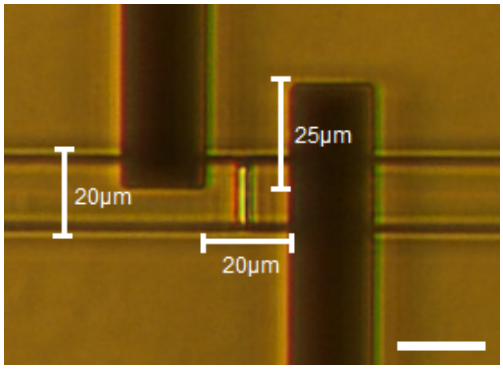

(a) Planar electrode design 1.

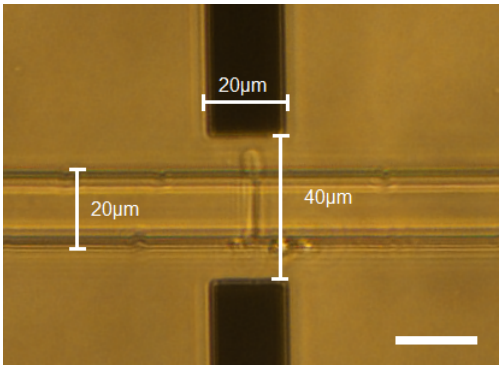

(b) Planar electrode design 2.

Figure 3.2: The two electrode designs. The electrode width is 20 µm and the overlap of the electrodes in the first design is 25 µm (scale bars are 20 µm)

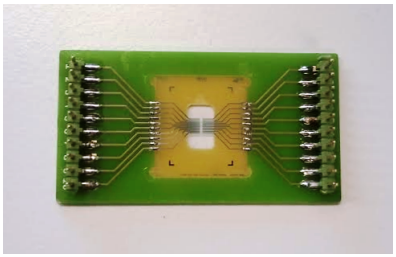

Figure 3.3: The PCB-glass set-up.

3.3 Sample preparation

Spermatozoa were obtained from KI Twente at a concentration of $20 \cdot 10^6$ cells per ml. For cell trapping experiments, a lower concentration of spermatozoa is desired. First the semen was vortexed, to get an even distribution of cells in the liquid. 50 µl semen was then mixed with 950 µl sperm medium. This gives a concentration of $1 \cdot 10^6$ spermatozoa per ml. Before using the prepared sample, it was be vortexed again, to reduce the amount of clustered cells. The semen and sperm medium were stored at 17°C. The sample was prepared before each experiment.

3.4 Single cell trapping

In all experiments on chip a Nemesys low pressure standard edition pump (Model NEM-B002-02 D) equipped with two Hamilton 100 µl syringes (Model 1710 N SYR, Cemented NDL, 22s ga, 2 in, point style 3) was used to draw the liquid through the channels. For the visualization of cells during the trapping and staining experiments on chip, a Nikon TE2000U Inverted Fluorescence Microscope was used. In Figure 3.4 the chip on the stage of a microscope is shown.

The syringes are connected to glass capillaries (ID 100 µm, OD 360 µm), which are connected to flexible tubing. This flexible tubing is inserted in the 1 mm inlets of the chip. To keep the chip in place, the glass substrate or PCB is taped to the microscope stage. The liquids are drawn through the channel by setting the syringe pump to a negative flow. For the 1 µm chip, a flow rate of 0.05 µl/min was used for the cell containing channel and 1 µl/min for the trapping channel. The 1.5 and 2 µm chips used flow rates of 0.75 and 0.5 µl/min for the trapping channel, while keeping the 0.05 µl/min for the cell containing channel. The larger suction of the trapping channel causes a pressure difference. This causes liquid to flow through the side channel. When the liquid is forced through the side channel, a spermatozoon is dragged along and sucked into the trap.

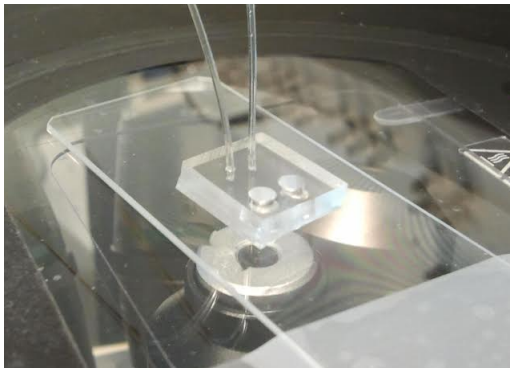

Figure 3.4: Chip on the microscope stage.

3.5 Viability staining on and off chip

For viability staining, SYBR 14 was diluted 2000x and PI 40x in the prepared semen sample (section 3.3). This solution was incubated for 10 minutes at room temperature and was then observed through a fluorescence microscope (EVOS FL Cell Imaging System).

For the viability staining on chip, the cells are first captured in the chip described in section 3.4. The SYBR/PI solution is then flowed through the channel, while the flow rates are kept at 0.5 µl/min and 1 µl/min. After the channels are completely filled with the dye mixture, the flow in the channels is stopped. After 10 minutes of incubation, the tubing is cut and the chip is visualized by the EVOS fluorescence microscope. The dye mixture is kept in the channel to observe the effect of PI on the cell viability.

3.6 FISH staining

3.6.1 FISH staining off chip

FISH staining was performed on four slides containing fixated spermatozoa. The semen sample was prepared as described in section 3.3 and was first exposed to a 37°C KCl solution. This solution is hypotonic, which inflates the cells. The cells were then fixated by adding Carnoy's fixate (Methanol:Acetic Acid, 3/1). For convenience, the location of the cells was marked with a diamond-tipped pen.

The slides were washed, dehydrated and further decondensated by a 37°C DTT solution. This solution breaks down the cell membrane and extracts the DNA from its protective proteins. Afterwards, the slides were washed and again dehydrated in the same manner.

The probe mixture was then added to the sample on the glass slide, followed by the denaturation (at 74°C) and hybridization (at 37°C) of the DNA and probe. The slide was then washed, where it was placed in a jar with 74°C 0.4X solution for 2 or 3 minutes. After washing the non-specific probe away, the slide was rinsed and air-dried.

To protect the fluorescent probe from photobleaching, Vectashield was pipetted onto the cells. The Vectashield can be used with or without the addition of DAPI as counterstain. The stained

cells were visualized with an EVOS FL Cell Imaging System. The detailed protocol can be found in Appendix A.2.

3.6.2 FISH staining on chip

FISH staining was performed several times on trapped cells in a chip. After the cells were trapped according to section 3.4, FISH staining on chip was peformed. As long as the cells were not fixated, the flow rates were kept at 0.5 µl/min and 1 µl/min. The cells were decondensated in 37°C KCl (0.075M) and fixated in Carnoy's fixate. The cells were then washed, dehydrated and further decondensated by a 37°C DTT solution. The DTT was flowed through with a pulsating flowrate, to ensure that the liquid reaches the desired temperature. Afterwards, the cells were washed and again dehydrated. Before the 74°C denaturation step, the wells of the chip were covered with parafilm. During the denaturing step, the parafilm melted to the glass/plastic substrate, sealing the wells. After the addition of the probe and the denaturation step, the complete mobile part of the set-up (which includes the tubing and syringes) was put into a 37°C hybridization chamber and left overnight (for shorter incubation periods, a 37°C hot plate was used). The set-up was then reinstalled, the parafilm was removed and the washing steps were performed. For the 74°C washing step, the chip was moved onto a 74°C hot plate, while no flow was present. Finally, Vectashield was flowed through the channel, the tubing was removed and the inlets were sealed with a coverslip.

For the 37°C DTT step of the FISH protocol, a the microscope hot plate was used. This plate could be placed inside the microscope while the chip could still be seen. The hot plate is made by Tokai Hit (model MATS-U505R30), which is made for the Nikon TE2000U Microscope. The maximum temperature that the plate can reach, is 50°C. For the 74°C denaturation and washing steps, an external Ika RET hot plate was used. The hot plate (IKA Works L005201 Ret Basic Hot Plate Stirrers Stainless Steel Plate Kit) has a maximum temperature of 340°C. For fluorescence imaging, an EVOS FL Cell Imaging System was used.

3.7 Impedance analysis

The impedance was measured with the use of a Zurich Instruments HF2IS (high-frequency, 2 inputs) impedance spectroscope. A 4-terminal measurement was performed, to eliminate the impedance of the wiring and contacts. The frequency sweep was performed between 100Hz and 5MHz. Two amplifiers, the HF2TA Current Amplifier and the HF2CA (Zurich instruments), were used to amplify the vltage and current separately. The set-up is illustrated in Figure 3.5. The recorded data was processed in Matlab (v2013b).

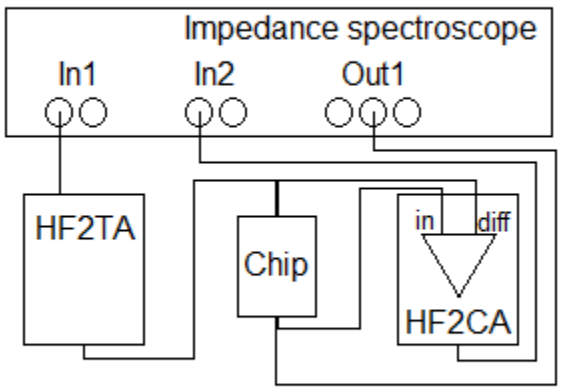

Figure 3.5: The set-up for the impedance measurements.

Chapter 4

Results and Discussion

4.1 Chip fabrication and set-up

Three different chip set-ups were designed to find an efficient method for single trapping of spermatozoa.

In **PDMS chip set-up 1** (Figure 4.1a), liquid was inserted through inlets 1 and 2. Inlets 3 and 4 were connected to a small waste container to catch the liquid. All inlets were made with a 1 mm pen, which forms a tight connection with the inserted tubing. To gain precise control over the pressure and flow rates, small volumes syringes were used. Due to the fact that liquid was pushed inside the channels, small pieces of PDMS where introduced inside the channels. Therefore, this debris was formed by the insertion of the tubing, which damaged the PDMS inlets. This method and set-up was therefore discarded.

With the **PDMS chip set-up 2** (Figure 4.1b), the liquid was not pushed in, but drawn through the channel by suction. Inlet A was made using a 3 mm pen; this large diameter was chosen to prevent the formation of air bubbles when pipetting the liquid in the inlet. Inlet 3 was closed, while inlets 1 and 2 were both connected to a syringe to provide suction. Exchange of liquids in inlet A was performed by using a fiberless tissue to suck up the remaining liquid and a pipette, to add the new liquid to the inlet. Because the second chip set-up used suction, introduction of PDMS debris was prevented. Furthermore, closing inlet 3 was not necessary, because a large flowrate from the syringe connected to inlet 2 was enough to provide a sufficient pressure difference and to create a fluid flow between the main channels. A disadvantage of the second design is the fact that a droplet, which was placed on inlet 3, would flow over the PDMS into inlet A. The connection of the droplets caused mixing of the liquids, introducing cells in the other channel.

Also, **PDMS chip set-up 3** (Figure 4.1c) was used, where inlets A and B were punched with a 3 mm pen. Both inlets were filled with the desired liquid, while inlets 1 and 2 were each connected to a syringe to provide suction. A fiberless tissue and a pipette were again used to exchange liquids. Increasing the size of inlet B in the third design prevented the mixing of liquids. This set-up was used for all further experiments.

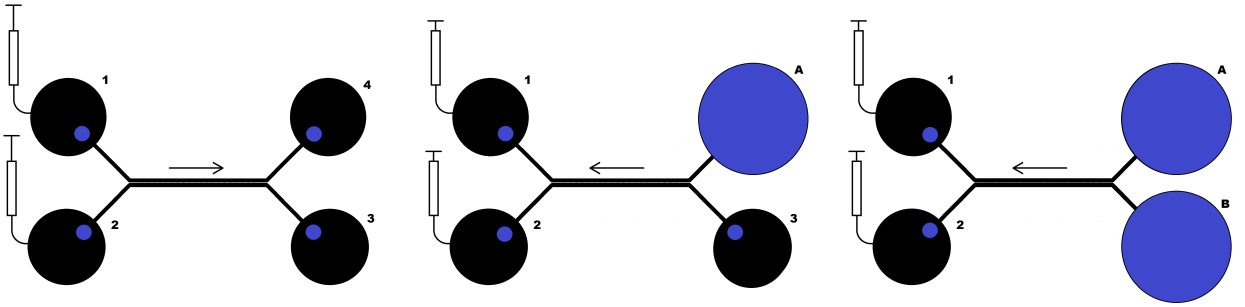

(a) 1st PDMS chip set-up. All inlets are made with a 1 mm pen.

(b) 2nd PDMS chip set-up. Inlets 1, 2 and 3 are made with a 1 mm pen, inlet A is made with a 3 mm pen.

(c) 3rd and final PDMS chip set-up. Inlets 1 and 2 are made with a 1 mm pen, inlets A and B with a 3 mm pen.

Figure 4.1: Three PDMS chip designs. Liquids are pushed through the channel in set-up 1 (a) and drawn through the channels by suction in set-ups 2 amd 3 (b and c). The flow directions are indicated with an arrow.

Because set-up 2 and 3 make use of suction, the amount of dead volume in inlets 1 and 2 is not important. The wells however had to be punctured such that they are connected to the channels, to reduce the dead volume. Exchanging fluids using a fiberless tissue and a pipette is a simple procedure, which provides complete control over the fluid composition within the channels.

4.2 Cell trapping

Hydrodynamic cell trapping experiments were performed using PDMS chips with three different cell trap heights (1, 1.5 and 2 μm) to find the optimal trap dimensions for single cell entrapment. Per trap height, three experiments were performed to investigate the trapping capacity (Table 4.1).

The percentage of cell trapping achieved with the 1, 1.5 and 2 μm trap heights were 43%, 47% and 27%. For increasing trap heights, more multiple trappings ocurred. In some cases, more than four spermatozoa could be caught in a 2 μm trap (Figure 4.2). When the trap height was increased, an increased number of cells was also able to be caught head-first instead of tail-first (Figure 4.3). The yield of single cell trappings was around 50%. Chip to chip differences were caused by fabrication artifacts. The chip with 1 μm channels was chosen for further experiments, because it gave the smallest chance of multiple cell trapping, which is undesirable for single cell analysis.

The trapping sites at the start of the main channel generally caught less spermatozoa than those at the end of the main channel. This was caused by the pressure gradient in the channels. Suction was used on two inlets to draw the liquid and cells through the channels. This suction was larger in the channel that did not contain the cells, which caused a pressure difference in the channels, drawing the fluid through the traps. For the traps at the end of the channel, closest to the outlets, the pressure drop was the highest. Therefore, a higher capture yield was observed for traps close to the outlets.

Table 4.1: Trapping rates for chips with trapping heights of 1, 1.5 and 2 µm respectively. Larger trap heights captured more spermatozoa, but had less single trappings.

Channel height	Single cells		Multiple cells		Empty channels	
1 µm		9		0		11
		10		1		9
	43%	7	2%	0	55%	13
1.5 µm		11		2		7
		9		2		9
	47%	8	12%	3	42%	9
2 µm		7		9		4
		3		14		3
	27%	6	60%	13	13%	1

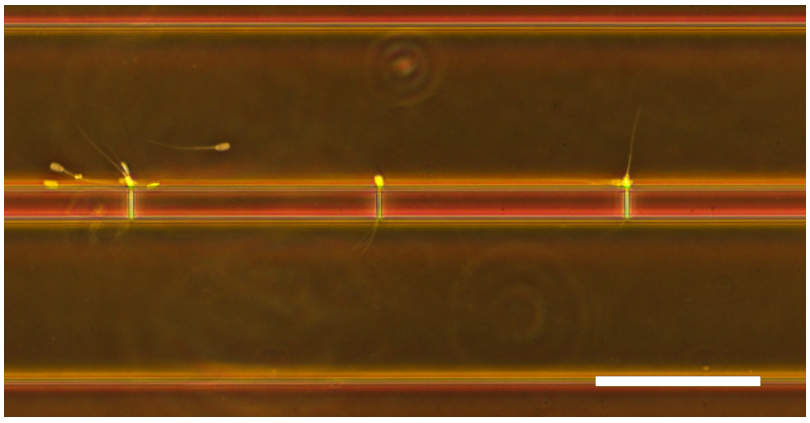

Figure 4.2: Multiple cell trapping in 2 µm traps. The two traps on the right have two cells each, while the one on the left has trapped at least four spermatozoa. (15x, scale bar is 100 µm)

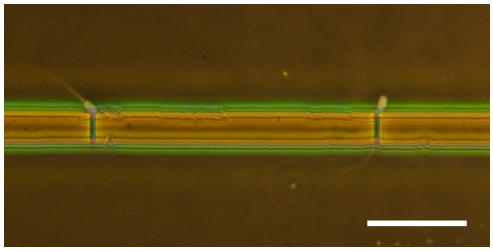

Figure 4.3: Sideways trapping (left) and trapping by tail (right) in 1.5 µm traps. (15x, scale bar is 50 µm)

Spermatozoa tended to stick to the glass in some experiments (see Figure 4.4). This was reduced by the use of fresh sample (dead cells stuck more to glass than viable cells) and larger flow rates. An antistick coating (PLL-g-PEG) was used, but this reduced the capturing rates of the spermatozoa in the preferred 1 µm chip by more than 50%.

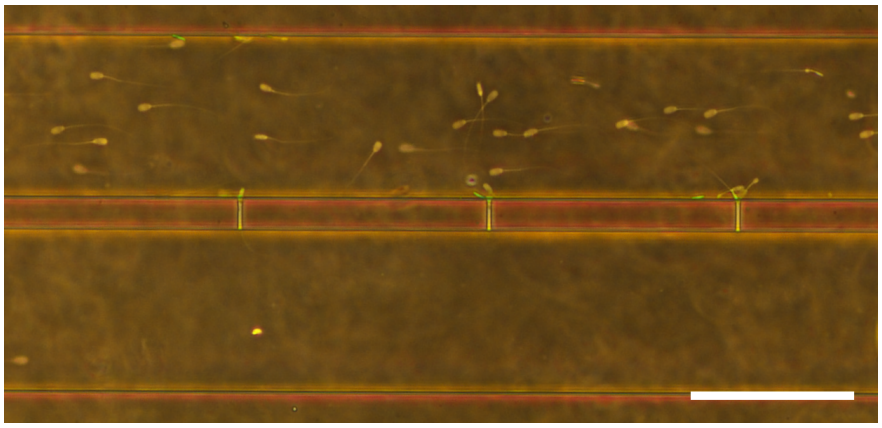

Figure 4.4: Dead cells sticking to the glass of the chip. (10x, scale bar is 100 µm)

4.3 Viability staining

Viability staining was performed on and off chip as described in section 3.5, to investigate the viability of spermatozoa.

4.3.1 Viability staining off chip

Viability staining was performed at the start of the project using of the dyes SYBR 14 and Propidium Iodide. SYBR 14 is able to permeate the cell membrane and bind to the DNA of a viable cell, wheras PI accumulates in the nucleus when the membrane is permeated. PI has a larger binding affinity to DNA. SYBR 14 thus stained viable spermatozoa, while PI stained dead spermatozoa, as it excludes the SYBR 14. SYBR 14 and PI emitted a green and red fluorescence respectively (see also Appendix B.1). The results of the staining are clearly seen in Figure 4.5. After 15 minutes incubation in the staining solution, almost all spermatozoa were viable and showed a green fluorescence. As the incubation time increased, the cells died one by one due to the toxic concentration of PI, showing a red fluorescence. After 30 minutes of incubation, all cells were red.

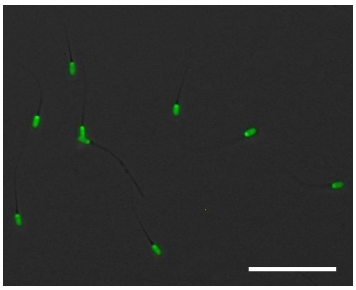

(a) Viable spermatozoa

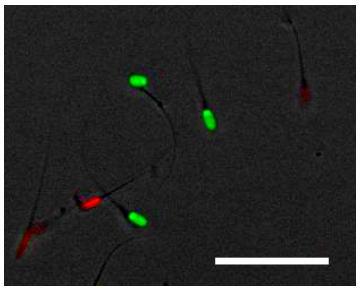

(b) Approximately half of the cells have died

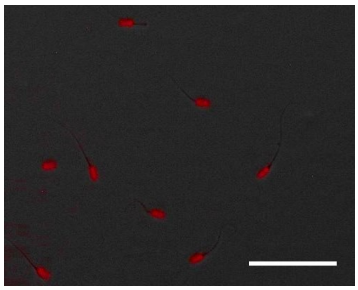

(c) Dead spermatozoa

Figure 4.5: Viability staining; the cells were viable at the start of the staining (a), but after prolonged exposure to the toxic PI, the cells were observed to die one by one (b). After 30 minutes, all cells had died (c). (20x, scale bars are 50 µm)

4.3.2 Viability staining on chip

Viability staining was performed on chip after capturing the cells on chip as described in section 3.4. This method allowed controlled trapping of the spermatozoa, keeping most of the spermatozoa alive. Figure 4.6 shows the death of a cell due to exposure to a toxic concentration of propidium iodide. The PI replaced the SYBR 14 when the cell dies (for the dyes, see Appendix B.1). Conditions and microscope settings during imaging were kept constant.

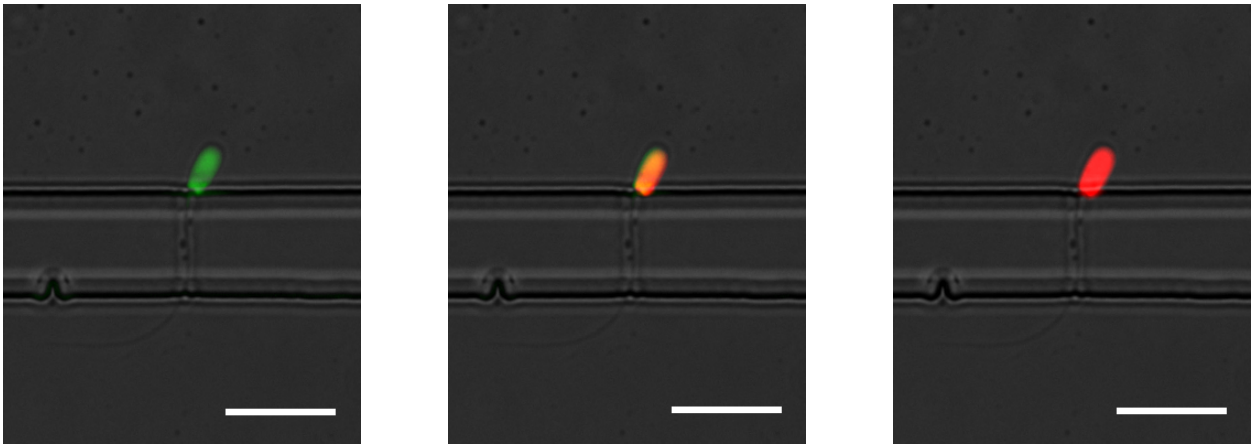

(a) Trapped cell after 15 minutes of exposure to the SYBR 14, PI mix.

(b) Trapped cell during cell death, after approximately 20 minutes of exposure. Both red and green fluorescence are visible, the PI is replacing the SYBR 14.

(c) Trapped cell after 25 minutes of exposure to the SYBR 14, PI mix. The PI has completely replaced the SYBR 14.

Figure 4.6: The exposure to a large concentration of PI caused the cell death of a trapped cell within 30 minutes. (40x, scale bars are 20 μm)

4.4 FISH staining

FISH staining was performed on and off chip as described in section 3.6. Several time steps were varied to obtain results with specific staining of the X and Y chromosomes.

4.4.1 FISH staining off chip

FISH staining was performed on four slides to get familiar with the protocol. The DTT step and the post-hybridization washing step are critical according to previous reports. Experiments were carried out using DTT steps of 15 and 25 minutes and washing steps of 2 and 3 minutes. The time steps are shown in Table 4.2. After the FISH staining, 3 slides were also stained with DAPI.

Table 4.2: Time steps for the FISH experiments.

Slide	DTT time step (min)	Washing time step at 74°C (min)	DAPI
1	15	3	yes
2	15	2	yes
3	25	3	yes
4	25	2	no

The slides that were exposed to a 3 minute washing step, only showed the red Y probe. On the slides with the 2 minute washing step, both probes were visible. It appears that a washing step of 3 minutes washed away the X probe. A washing step of 2 minutes seems to have cleaned the cells from nonspecific staining, but did not wash away the specific staining on both the X and Y chromosome. This difference is visible in Figures 4.7a and 4.7b. One slide was not stained with DAPI. These cells were visualized using phase contrast (Figure 4.8). As an advantage, the X chromosome staining in these cells was clearer compared to DAPI stained cells, in which the fluorescent response of the specific staining is negatively influenced by spectral overlap with the DAPI fluorophore.

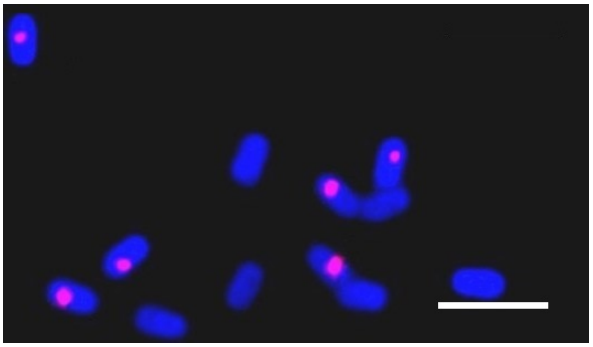

(a) A 15 min DTT and a 3 min washing step. The Y probe is visible, but the X probe seems to have been washed away.

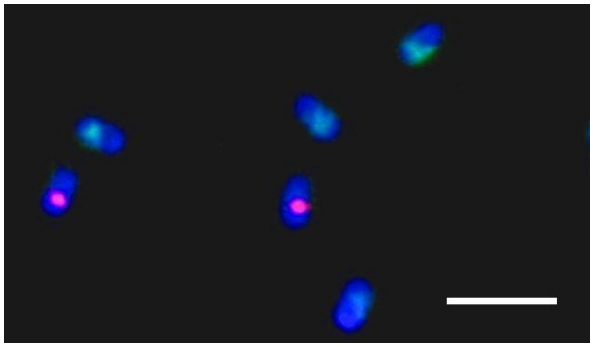

(b) A 15 min DTT and a 2 min washing step. Both the X and Y probe are visible, the X probe is more decondensed because of its larger size and also less clear due to the additional staining with DAPI.

Figure 4.7: FISH staining with DAPI (40x, scale bars are 20 µm)

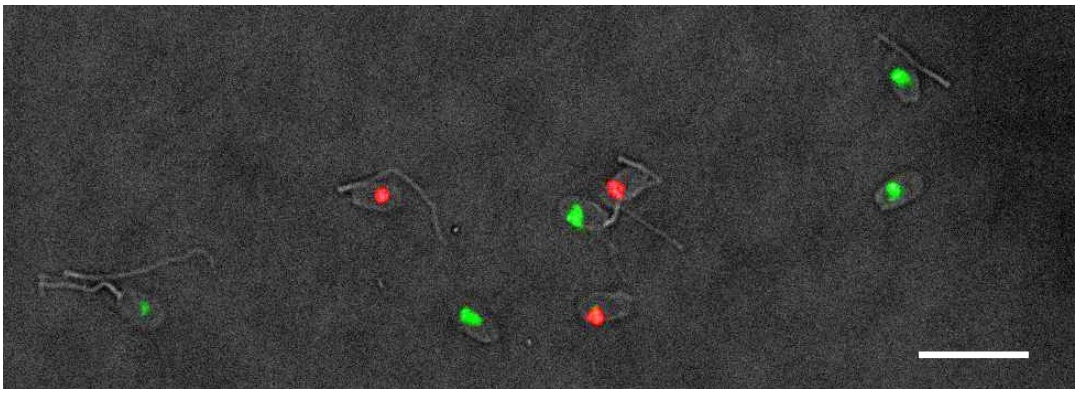

Figure 4.8: FISH staining (25 min DTT, 2 min wash). The cells were not stained with DAPI, because the cells were visualized by phase contrast. Both the X and Y chromosome are visible. (40x, scale bar is 20 µm)

4.4.2 FISH staining on chip

FISH staining was performed on cells trapped on a chip according to the FISH staining on chip protocol in Appendix A.4. Several experiments were performed to optimize the DTT, washing and hybridization steps. The different durations of the steps are shown in Table 4.3

Table 4.3: Time steps for the FISH on chip experiments.

Experiment	Hybridization time (h)	DTT time step (min)	Washing time step at 74°C (min)
1	2	15	0.5
2	16	25	1.5
3	16	17	2
4	16	20	2
5	16	20	2.5
6	4	20	2.5

DTT

The spermatozoa were exposed to a DTT solution, which dissolves the cell membrane and breaks the disulfide bonds between protamines to unravel the tightly packed DNA. To investigate the effect of the exposure time to DTT, the cell nuclei, and specifically the DNA within the nuclei, were visualized with DAPI. This dye shows the edges of the cell, indicating how much it has fallen apart. The cells were not decondensated enough after 15 minutes of exposure to DTT. A time step of 25 minutes led to too much condensation, resulting in cells invisible by phase contrast. A DTT step of 20 minutes left the cell structure intact, but opened the membrane enough to allow hybridization of the probe and DNA. The results of the exposure times are shown in Figure 4.9.

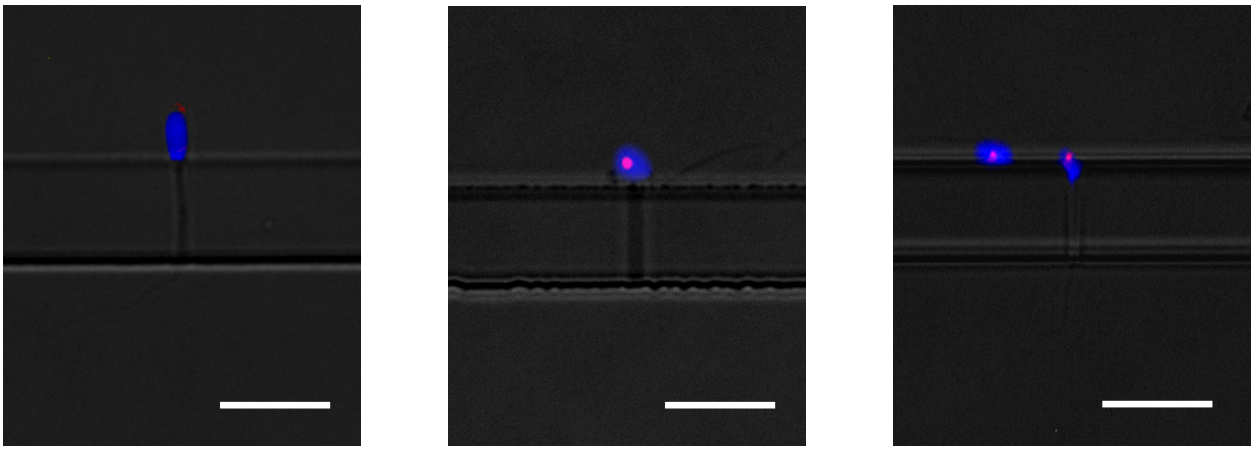

(a) Trapped spermatozoon after a DTT step of 15 minutes (exp 1)

(b) Trapped spermatozoon after a DTT step of 20 minutes (exp 2)

(c) Trapped spermatozoa after a DTT step of 25 minutes (exp 4)

Figure 4.9: Visualization of FISH staining after three DTT time steps (15, 20 and 25 min). (40x, scale bars are 20 µm)

Washing step at 74°C

Several washing time steps were tested in the FISH staining experiments on chip. A washing step of 2 minutes, which was the optimal washing time for FISH staining on slide, was not enough for FISH on chip. There was nonspecific staining on the cell membrane and PDMS debris. After 2.5 minutes, the nonspecific staining was completely removed from the cells (see Figure 4.10).

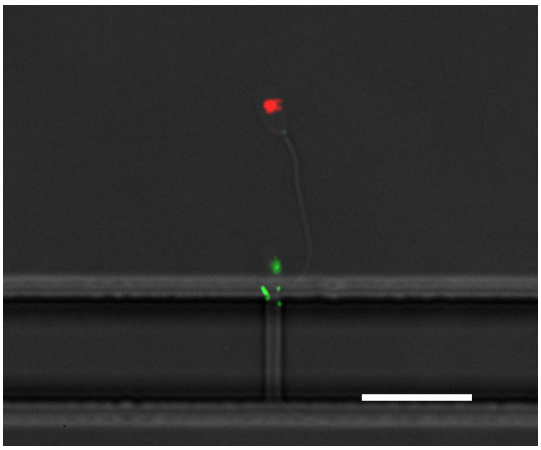

(a) Cells after a washing step of 2 minutes (exp 4).

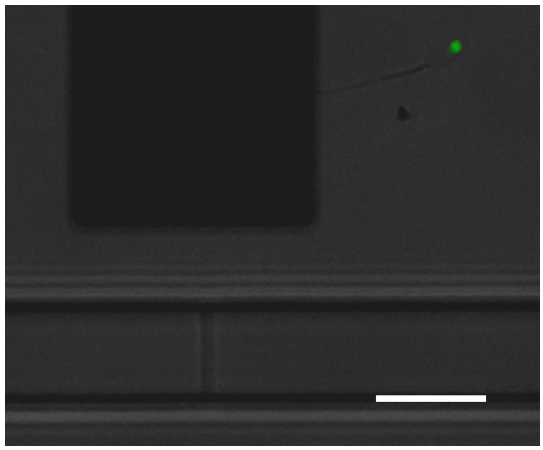

(b) Cell after a washing step of 2.5 minutes (exp 5).

Figure 4.10: Visualization of FISH stained spermatozoa after two washing steps (2 and 2.5 min). (40x, scale bars are 20 µm)

DAPI

As already mentioned in section 4.4.1, DAPI binds to the DNA in the spermatozoa, increasing the visibility of the nucleus. However, the visibility of the green probe is negatively affected. Due to spectral overlap, both the DAPI and the X chromosome fluorophore emitted a green signal. In Figure 4.11 two spermatozoa with and without DAPI are shown.

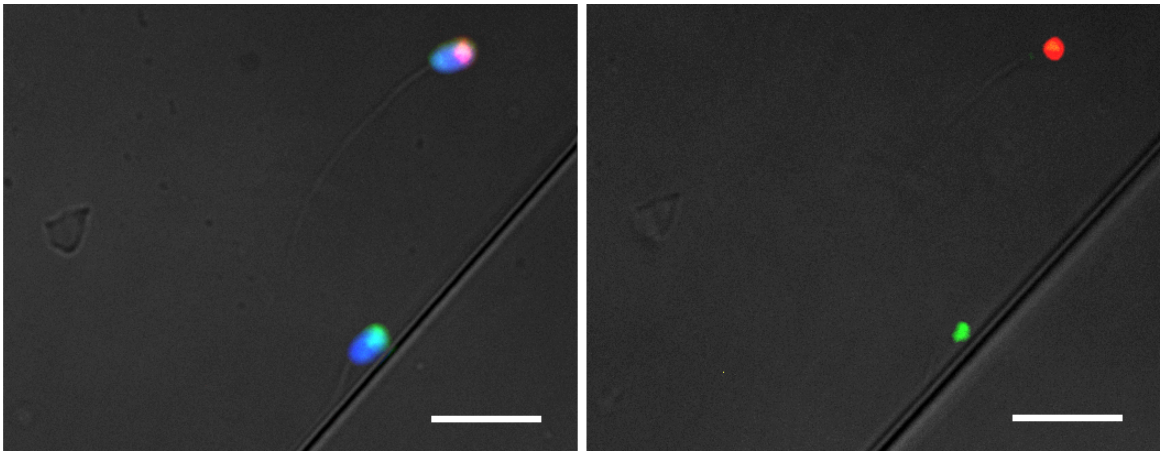

Figure 4.11: Cells in the first part of the channel from 3rd attempt at FISH on chip. The DAPI was added as it makes it easier to find and identify the cells, but the spectral overlap of DAPI and the green probe reduces the visibility of the green probe. (40x, scale bars are 20 µm)

The drying steps in the FISH protocol caused problems in some chips. The protocol was also tried without any drying steps, which gave no significant differences with the protocol with the drying steps. The drying steps were thus removed from the protocol.

Final results

Figure 4.12 shows the final results of the fifth experiment. FISH staining was performed on a chip with microelectrodes, to investigate the effect of the microelectrodes on the FISH staining results. In Figure 4.12, it can be seen that the electrodes did not influence the results. FISH staining can therfore be performed on spermatozoa after they have been analysed with impedance spectroscopy. The results from experiment 6 are not shown, because there was no staining of the cells or PDMS. A possible explanation is the short hybridization time of the probe. The hybridization is a slow diffusion based process, which may need more than four hours. Therefore, the optimal conditions for a succesful FISH staining one spermaztozoa are a DTT step of 20 minutes, a washing step of 2.5 minutes and an overnight hybridization.

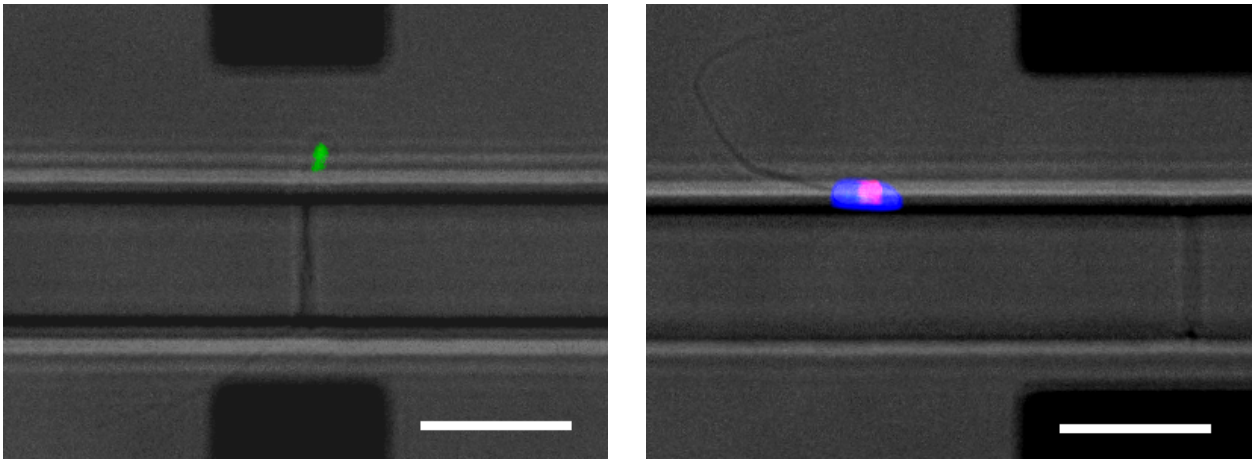

(a) **(b)**

Figure 4.12: Results from experiment 5. After staining, the platinum electrodes are unchanged and the FISH staining results were succesful. No nonspecific staining was observed. (40x, scale bars are 20 μm)

4.5 Impedance analysis

Several impedance measurements were performed on empty traps and on traps which were filled with 11 μm beads and spermatozoa. The behaviour of the system was also modelled and simulated to predict its dielectric response.

4.5.1 Electrode orientation

The impedance was recorded as decribed in section 3.7, using the electrode designs described in section 3.2. Electrode designs 1 and 2 were tested. The electrodes of electrode design 2 were positioned in such a way that they would measure through the trap. A filled trap however had such a high impedance, that the electric field would go through the empty neighboring traps, instead of through the desired trap. The second design could therefore not be used for single cell measurements. Design 1 did not suffer from this problem. In this orientation, the electric field does not go through the channels. Therefore, this design was used in further experiments.

4.5.2 Simulations

To gain insight in the electrical properties of the microfluidic set-up, an ECM was constructed. Bjorn de Wagenaar simulated the dielectric behavior of an empty trap and a trap with a spermatozoon in both Milli-Q and sperm diluent.

Foster and Schwan's model was used for the construction of the ECM. A spermatozoon differs from normal cells in several ways. It has a stronger membrane and inside the head a large amount of the cytoplasm is DNA. A sperm cell also has a tail that is 5 to 10 times the size of the head. The head of a spermatozoon consists of a cell membrane and cytoplasm (the tail is not considered in this work). The cell membrane is composed of a lipid bilayer. Within this cell membrane, the cytoplasm is contained, which consists of a large amount of negativily charged DNA. A spermatozoon can therefore also be modelled by a capacitor and a resistor.

Figure 4.13 shows the ECM's for an empty trap and a trap with a spermatozoon. In the model for the empty trap, the medium in which the cell was suspended, was modelled as a parallel resistor and capacitor. The double layer of the electrodes and medium was modelled as two capacitors. These two capacitors are placed in series with the parallel resistor and capacitor of the medium. A parasitic capacitor is placed in parallel to this (Figure 4.13a).

In the model for the trap with a cell, two capacitors and a resistor in series were placed parallel to the medium resistor and capacitor (Figure 4.13b).

Figure 4.14 shows the impedance and phase plots for the simulations of these models. At low frequencies the double layer capacitance is completely charged. As the frequency increases, the capacitors have less time to be charged, allowing more current through. This causes the first drop in impedance in the impedance spectrum of the empty trap. When the impedance of the double layer capacitance is lower than the impedance of the medium resistance, the medium resistance becomes the limiting factor. Therefore, a resistive plateau is visible in the impedance plot. At even higher frequencies, the capacitance of the medium and the parasitic capacitance become dominant. The impedance of these capacitors decreases until it is lower than that of the medium resistance. As the current takes the path of the least resistance, the current then goes through the medium and parasitic capacitors. Therefore, a second drop in impedance is visible at larger frequencies.

When a cell is measured, the impedances of the double layer and membrane go down until the resistances of the medium and the cell become dominant. The cell however has a lower impedance than the medium due to the charged interior. The electric field always goes the path of the least resistance, so when a cell is measured at high frequencies, the current goes (partly) through the cell. Therefore, a drop in impedance is seen at the frequency range of the resistive plateau.

The impedance drop is larger for less conductive mediums, as there is a larger difference in impedance between the medium and the cell. In Figure 4.14, this effect is shown in the impedance plot. A phase plot is also shown, where capacitive behavior causes a negative phase shift, while resistive behavior increases the phase.

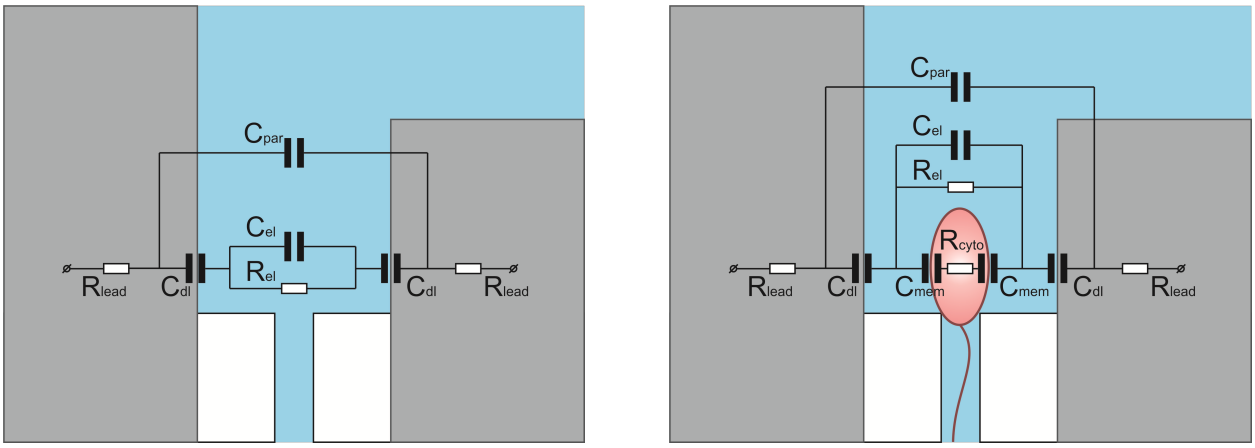

(a) ECM for an empty trap **(b)** ECM for a filled trap

Figure 4.13: Equivalent circuit models for a trap with (b) and without (a) a spermatozoon (constructed by Bjorn de Wagenaar).

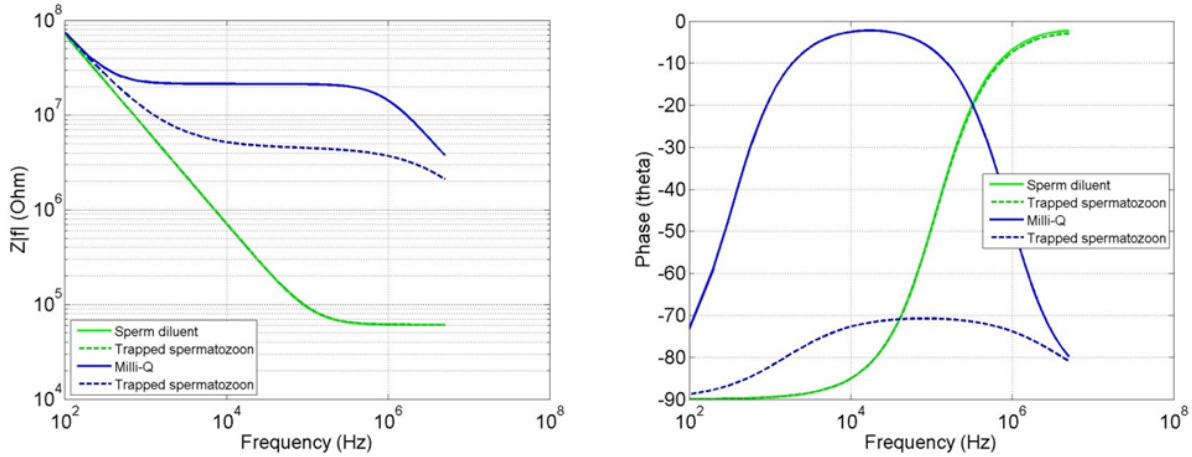

(a) Impedance **(b)** Phase

Figure 4.14: Spectra of the ECM with sperm diluent and Milli-Q, with and without a trapped spermatozoon (constructed by Bjorn de Wagenaar).

4.5.3 Characterization

For the characterization of the chip, impedance measurements were performed for liquids with different conductivities and for different measurement areas.

Liquids with a higher conductivity shifted the spectrum down and to the right. A higher conductivity is paired with a lower resistance. The resistive plateau that is caused by this resistance is visible at higher frequencies, when the impedance of the double layer capacitance is lower than the resistance of the medium. The parasitic capacitance is also seen at higher frequencies in the spectrum due to the lower impedance of the medium. In Figure 4.15, the lowering of the plateau and the shifting of the phase are shown as a result of increasing conductivity.

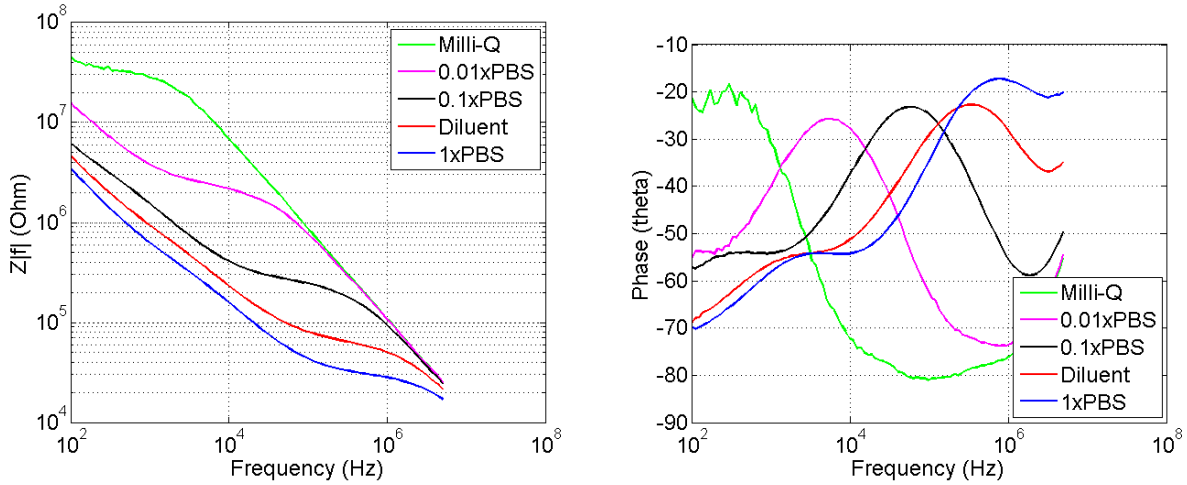

(a) Impedance **(b)** Phase

Figure 4.15: Impedance and phase spectra for liquids of increasing conductivity.

In Figure 4.16, it can be seen that the impedance goes down for a larger measurement area. A larger area gives a larger measurement volume, which contains more conductive electrolyte. A larger amount of electrolyte causes a lower impedance. The impedance also goes down for a larger trap height, although this effect is smaller. A difference of 1 μm in the measurement area with the same trap height (blue solid and dashed lines) has a much larger effect than a different trap height for the same measurement area (green and blue dashed lines).

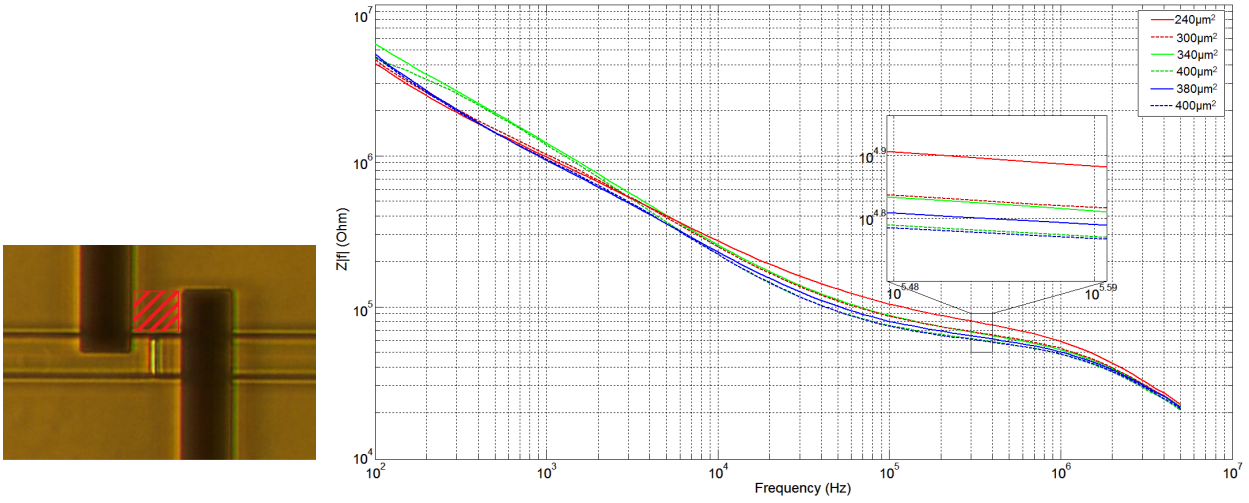

(a) Measurement area **(b)** Impedance

Figure 4.16: Measurements in sperm diluent for different measurement areas. The green, red and blue lines are for the chips with 1, 1.5 and 2 μm trap heights respectively.

In the measurements, the parasitic capacitance becomes dominant at a lower frequency than for the simulations. The behavior of the system is also never completely resistive. There is also a second resistive region visible in the measurement data, which is not seen in the simulations. The behavior of this region is explored in section 4.5.5.

4.5.4 Beads and cells

Impedance measurements were performed on cells and 11 μm beads in sperm diluent and Milli-Q. During the experiments, a control measurement was done by sweeping the traps while they were still empty. After cell/bead trapping, the traps were again sweeped. If the cells/beads could be expelled, a second control measurement was done. This was done to take into account the differences in ion concentration due to the drift of the medium.

Beads

Plastic beads are insulators, and do not allow current to pass over the entire frequency range. The beads showed a larger impedance over the complete frequency range, with some irregularities at frequencies under 1 kHz. The impedance difference caused by the beads increased with a factor 10 for measurements in Milli-Q compared to measurements in sperm diluent. The beads did not have a large influence on the phase spectrum (Figure 4.17).

Cells

For the sperm cell measurements, an increase in impedance was seen at low frequencies, while a decrease was visible at higher frequencies (Figure 4.18). At lower frequencies, the current is forced around the cell by the cell membrane, while at higher frequencies, it is possible measure through the cell membrane and see the more conductive interior of the cell.

The cells displayed similar behavior for the real measurements and the simulations. The phase became more negative, although it was not as extreme as in the simulations, and there was also a small frequency shift to the right. In the plots, the earlier occurence of the parasitic capacitance is also visible.

In Milli-Q the cells had a much larger effect than in sperm diluent. The drop in impedance was larger, which was caused by the large difference in impedance between the low conductive Milli-Q and the high conductive interior of the cell.

The frequency of the impedance crossover was fairly consistent for the diluent measurements, but no relation between the amount of cells and the crossover frequency was found. The presence but not the amount of membranes determined the crossover frequency. The integrity of the membrane is suspected to influence the crossover frequency.

The impedance difference was measured at the resistive plateau, where no relation was found between the amount of cells and the impedance drop. No differences in the impedance spectra were seen for cells that lay flat and those that lay on their sides. There were not enough measurements done in Milli-Q to compare the crossover frequency or the impedance drop in this medium. It was however seen that the crossover frequency lies at around 200 Hz and that the impedance drop was approximately 1.5 MΩ.

In Table 4.4, the crossover freqencies and the impedance difference at the resistive plateau are shown. The impedance difference was measured at the frequency with the most resistive behaviour (the largest phase in the phase plot). For the measurements in Table 4.4, this frequency was 0.8 MHz.

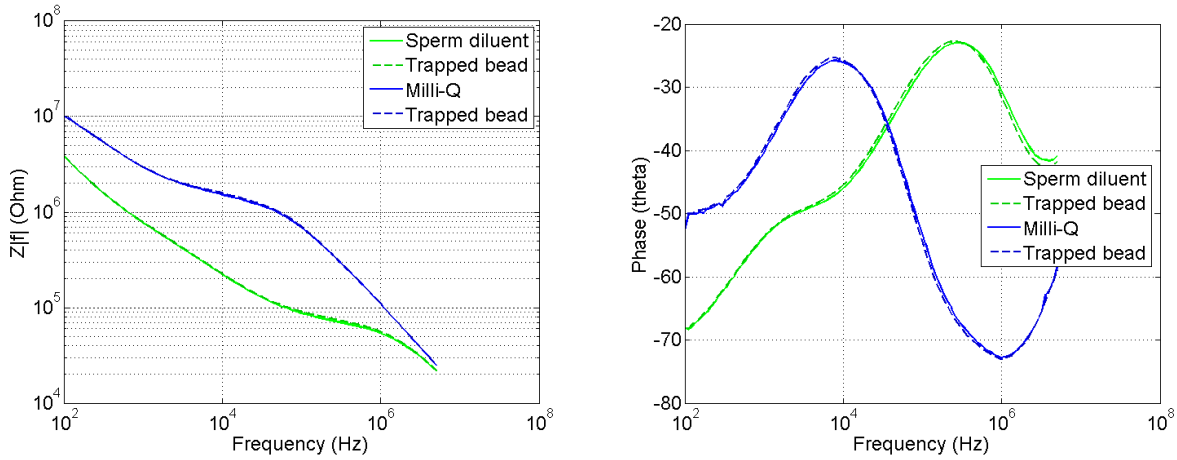

(a) Impedance **(b)** Phase

Figure 4.17: Spectra of an empty trap and a trap filled wit an 11 µm bead in sperm diluent and Milli-Q.

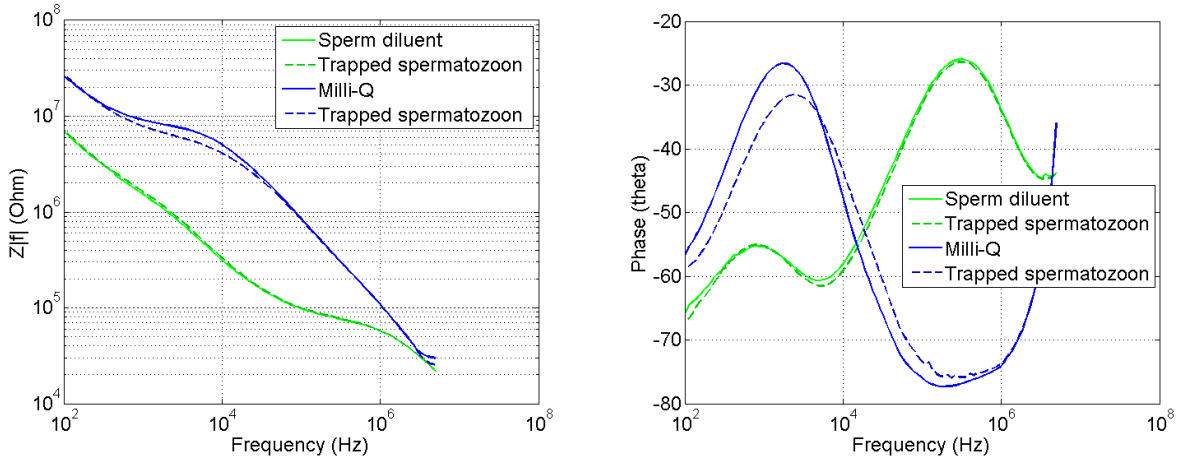

(a) Impedance **(b)** Phase

Figure 4.18: Spectra of an empty trap and a trap with a spermatozoon in sperm diluent and Milli-Q.

Table 4.4: Crossover frequencies and impedance differences at the resistive plateau for different cells in diluent (all measured in the same trap)

Number of cells	Crossover frequencies (Hz)	Impedance difference at $8 \cdot 10^5$ Hz (Ω)
1	$4.8{\cdot}10^4$	2164
1	$2.4{\cdot}10^5$	174
2	$4.6{\cdot}10^4$	1824
3	$5.1{\cdot}10^4$	1479

Comparison

The measurements on 11 µm beads were performed as a control for the measurements on spermatozoa. Figures 4.17 and 4.18 show the results for two measurements on beads and cells respectively.

The beads showed an increase in impedance over the complete frequency range. Conversely, the cells increased the impedance at lower frequencies, but caused a decrease at the resistive plateau. This drop in impedance suggests that the interior of the cell can be measured. Because the interior of spermatozoa mainly consists of DNA, the presence and probably the amount of DNA can be measured.

4.5.5 The influence of the trap

In the impedance spectra, a resistive behavior was visible at lower frequencies (Figure 4.19). This resistive behavior did not occur in the simulations, indicating that there was another factor that had an effect on the impedance. We suspect that part of the current goes through the trap to the other electrode. This can be seen as a leak resistance. This was investigated by looking at the phase plots of the impedance measurements for several measurement areas and trap heights.

In Table 4.5, the phase shift of this resistive plateau can be seen for different trap sizes and measurement areas. The last result of the 1 µm chip was disregarded, as it deviated substantially from the other results. There appeared to be more resistive behavior for smaller measurement volumes. The 1.5 µm channels showed more resistive behavior than the 2 µm channels, but that of the 1 µm channels was less resisitive than both. The two equal 1 µm measurement volumes had equal phase shifts (-58 ϑ).

For larger traps, it might be that it is easier for the current to go through the traps, leading to a lower resistance and a larger contribution to the impedance. The 1 and 2 µm traps seemed to confirm this suspicion, the resistive behavior increased for a larger trap height and the frequency shift that accompanies a drop in impedance confirmed the lower resistance of a larger trap. The 1.5 µm trap however showed different behavior, more research is needed to investigate this.

The influence of the trap occurs at low frequencies. It does not appear at the frequencies where the resistive plateau occurs, which are our frequencies of interest.

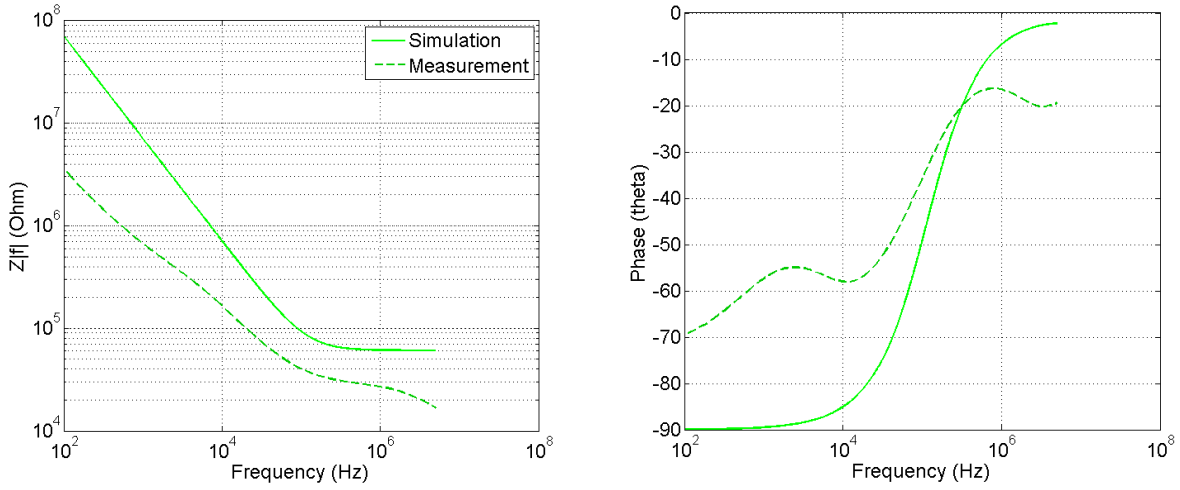

(a) Impedance **(b)** Phase

Figure 4.19: Impedance and phase spectra of the simulation and measurement of an empty trap.

Table 4.5: Magnitude and frequency of the phase shift of the unexpected resistive behaviour for various trap heights and measurement areas (measured in sperm diluent). The measurement marked with * deviated substantially form other measurements.

Trap height (µm)	Measurement area (µm^2)	Phase shift (ϑ)	Frequency (Hz)
1	340	-58	460
1	340	-58	798
1	360	-59	540
1*	400*	-45*	<100*
1.5	240	-51	1378
1.5	300	-53	1240
2	380	-54	1912
2	400	-55	1540

Chapter 5

Conclusions

In this project, we investigated single cell trapping, viability and FISH staining and the impedance behaviour on chip to create a platform for single cell analysis of spermatozoa.

Several PDMS chip designs where tested for optimal fluid throughput. A design that contained two large inlets and that made use of suction was chosen. The fact that suction was used, prevented the introduction of PDMS debris. The large inlets of the design prevented the formation of air bubbles and the mixing of fluids.

Three different trap heights were tested on their single cell trappig capacity. The 1 μm traps showed the largest amount of single cell trappings compared to multiple trappings with an average trapping yield of 43% vs. 2%. These traps tended to catch single cells with their tails in the traps. Conversely, the 1.5 and 2 μm traps caught spermatozoa head-first as well as tail-first. These larger traps sometimes caught more than four spermatozoa.

The viability staining on and off chip both turned out succesful. Prolonged exposure to the toxic concentration of PI caused cell death in both experiments. During the viability staining on chip, the death of a single cell could be monitored.

The FISH staining protocol was tested and adjusted. The results of the FISH staining showed that the 3 minute washing step of the original protocol was too long, resulting in washed away probe. The duration of the washing step was adjusted to 2 minutes.

The development of a protocol for FISH staining of spermatozoa on chip was succesful. Appropriate flow rates were chosen in such a way that cells could be caught and stained. Several untrapped spermatozoa were also fixated inside the channels to have a large population for the experiments. After several experiments, a DTT step of 20 minutes and a washing step of 2.5 minutes resulted in specific staining without too much dispersion of the fluorescent signal. The drying steps were also removed from the protocol.

Impedance analysis on trapped spermatozoa was performed in sperm diluent and Milli-Q. The impedance behavior of beads and spermatozoa was investigated. Preliminary results show that the presence of a spermatozoon in a microfluidic chip can be detected through impedance spectroscopy. Beads increased the impedance at the resistive plateau, while spermatozoa caused a drop in impedance at these frequencies. This drop in impedance suggests that the interior of the cell can

be measured. Because the interior of spermatozoa mainly consists of DNA, the quantity of DNA can probably be measured. The impedance difference caused by a cell increased with a factor 1000 when a Milli-Q instead of sperm diluent was used.

5.1 Recommendations

Several recommendations are proposed to increase the trapping efficiency and throughput and to improve the fluorescent stainings and electrical measurements.

- The yield of single cell trapping could still be improved. Chips without fabrication artifact could be made, as clean chips probably trap more spermatozoa.
- The viability experiments on chip could be repeated with a lower concentration of PI. A lower (non-toxic) concentration of PI would keep the cells viable for a longer time, while still allowing to monitor cell death.
- The FISH on chip protocol could be repeated for different hybridization times, to research if a shorter hybridization time is possible.
- An isotonic low conductive solution could be used for the impedance measurements of spermatozoa. This way, there is no difference in osmolarity, preventing cell death by inflation.
- More impedance measurements could be done for a better characterization of the chip and cells, as no conclusion could be drawn apart from their existence in the trap.
- Electrodes with a smaller measurement volume could also be designed, which would increase the influence of the spermatozoa on the field. The cell would occupy a larger fraction of the measurment volume, leading to relatively more electric field through the cell.
- Also, the viability and FISH staining protocols could be used in combination with impedance measurements. This way, realations between spermatozoa viability/sex and dielectric behavior can be found. It is suspected that the cell membrane integrity influences the crossover frequency, while the amount of DNA influences the impedance drop.

Bibliography

[1] Sudhir Roy. *Sperm sexing techniques and their applications*. 2010. URL: http://ahd.maharashtra.gov.in/pdf/mldb/sperm%20sexing.pdf.

[2] Vincent ter Beek. "Sex sorting technology could save time and money". In: *Pig Progress* 23.10 (2007), pp. 22–23. URL: http://www.pigprogress.net/PageFiles/27740/001_boerderij-download-PP5803D01.pdf.

[3] Overheid.nl. *Wet afbreking zwangerschap*. 2014. URL: http://wetten.overheid.nl/BWBR0003396/geldigheidsdatum_10-03-2014.

[4] "Preconception gender selection for nonmedical reasons". In: *Fertility and Sterility* 82, Supplement 1 (2004), pp. 232–235. ISSN: 0015-0282. DOI: 10.1016/j.fertnstert.2004.05.013. URL: http://www.sciencedirect.com/science/article/pii/S0015028204008921.

[5] C. O'Connor. "Genetic mechanisms of sex determination." In: *Nature Education* (2008), 1(1):25.

[6] Peter Chen. *Biology genetics*. 2007.

[7] N.A. Campbell et al. *Biology*. Global Edition. Benjamin Cummings / Pearson Education. ISBN: 9780321739759.

[8] Loes Irene Segerink. "Fertility chip : a point-of-care semen analyser". PhD thesis. Enschede, the Netherlands, Nov. 2011. URL: http://doc.utwente.nl/78340/.

[9] S. Bonet et al. *Boar Reproduction: Fundamentals and New Biotechnological Trends*. Springer, 2013. ISBN: 9783642350498.

[10] J. M. Cummins and P. F. Woodall. "On mammalian sperm dimensions". In: *Journal of Reproduction and Fertility* 75.1 (1985), pp. 153–175. DOI: 10.1530/jrf.0.0750153.

[11] V. Ingram. *Biology Hypertextbook*. 2006.

[12] A. Annunziato. "DNA packaging: Nucleosomes and chromatin." In: *Nature Education* (2008), 1(1):26.

[13] Undraga Schagdarsurengin. "Analysing the sperm epigenome: roles in early embryogenesis and assisted reproduction". In: *Nature Reviews Urology* 9 (2012), pp. 609–619. DOI: 10.1038/nrurol.2012.183.

[14] P. Atkins and J. de Paula. *Atkins' Physical Chemistry*. OUP Oxford, 2010. ISBN: 9780199543373.

[15] Winfried Wiegraebe. *Fluorescence*. 2014. URL: http://research.stowers-institute.org/microscopy/external/Technology/index.htm.

[16] M. Sauer, J. Hofkens, and J. Enderlein. *Handbook of Fluorescence Spectroscopy and Imaging: From Ensemble to Single Molecules*. Wiley, 2011. ISBN: 9783527633517.

[17] "Fluorescence microscopy". In: *Nature Methods* 2 (2005), pp. 910–919. DOI: 10.1038/nmeth817.

[18] Life Technologies. *Nucleic Acid Stains—Section 8.1.* 2014. URL: http://www.lifetechnologies.com/nl/en/home/references/molecular-probes-the-handbook/nucleic-acid-detection-and-genomics-technology/nucleic-acid-stains.html.

[19] C. O'Connor. "Fluorescence in situ hybridization (FISH)." In: *Nature Education* (2008), 1(1):171.

[20] Nation Master. *Fluorescent in situ hybridization.* 2007.

[21] Erik B. van Munster et al. "Difference in volume of X- and Y-chromosome-bearing bovine sperm heads matches difference in DNA content". In: *Cytometry* 35.2 (1999), pp. 125–128. ISSN: 1097-0320. DOI: 10.1002/(SICI)1097-0320(19990201)35:2<125::AID-CYTO3>3.0.CO;2-H. URL: http://dx.doi.org/10.1002/(SICI)1097-0320(19990201)35:2%3C125::AID-CYTO3%3E3.0.CO;2-H.

[22] Ilaria Natali. "Sperm Preparation Techniques for Artificial Insemination - Comparison of Sperm Washing, Swim Up, and Density Gradient Centrifugation Methods". In: *Artificial Insemination in Farm Animals.* Springer, 2011. DOI: 10.5772/713.

[23] K H Cui. "Size differences between human X and Y spermatozoa and prefertilization diagnosis." In: *Molecular Human Reproduction* 3.1 (1997), pp. 61–67. DOI: 10.1093/molehr/3.1.61.

[24] S Kaneko et al. "Separation of human X- and Y-bearing sperm using percoll density gradient centrifugation." In: *Fertil Steril.* 40.5 (1983), pp. 661–665.

[25] Shau-Ping Lin et al. "Separating X-Bearing Human Spermatozoa Through a Discontinuous Percoll Density Gradient Proved to Be Inefficient by Double-Label Fluorescent In Situ Hybridization". In: *Journal of Assisted Reproduction and Genetics* 15.9 (1998), pp. 565–569. ISSN: 1058-0468. DOI: 10.1023/A:1022590321986.

[26] B Alexander, G Mastromonaco, and WA King. "Recent Advances in Reproductive Biotechnologies in Sheep and Goat". In: *J Veterinar Sci Technol* 1.101 (2010). DOI: 10.4172/2157-7579.1000101.

[27] GE Seidel and DL Garner. "Current status of sexing mammalian spermatozoa". In: *Reproduction* 124.6 (2002), pp. 733–743. DOI: 10.1530/rep.0.1240733. URL: http://www.reproduction-online.org/content/124/6/733.abstract.

[28] UCSF School of Medicine. *Flow Cytometry and Flourescence-Activated Cell Sorting (FACS).* 2014. URL: http://missinglink.ucsf.edu/lm/molecularmethods/flow.htm.

[29] Johan Nilsson et al. "Review of cell and particle trapping in microfluidic systems." In: *Analytica chimica acta* 649.2 (2009), pp. 141–157. DOI: 10.1016/j.aca.2009.07.017.

[30] Dino Di Carlo, Nima Aghdam, and Luke P. Lee. "Single-Cell Enzyme Concentrations, Kinetics, and Inhibition Analysis Using High-Density Hydrodynamic Cell Isolation Arrays". In: *Analytical Chemistry* 78.14 (2006), pp. 4925–4930. DOI: 10.1021/ac060541s.

[31] Mengsu Yang, Cheuk-Wing Li, and Jun Yang. "Cell Docking and On-Chip Monitoring of Cellular Reactions with a Controlled Concentration Gradient on a Microfluidic Device". In: *Analytical Chemistry* 74.16 (2002), pp. 3991–4001. DOI: 10.1021/ac025536c.

[32] G Fuhr et al. "High-frequency electric field trapping of individual human spermatozoa." In: *Human Reproduction* 13.1 (1998), pp. 136–141. DOI: 10.1093/humrep/13.1.136.

[33] Timo A. Nieminen et al. "Physics of Optical Tweezers". In: *Laser Manipulation of Cells and Tissues*. Ed. by Michael W. Berns and Karl Otto Greulich. Vol. 82. Methods in Cell Biology. Academic Press, 2007, pp. 207–236. DOI: 10.1016/S0091-679X(06)82006-6.

[34] Jaclyn L. Nascimento et al. "Analysis of sperm motility using optical tweezers". In: *Journal of Biomedical Optics* 11.4 (2006), pages. DOI: 10.1117/1.2337559.

[35] J.-P. Frimat et al. "Make it spin: individual trapping of sperm for analysis and recovery using micro-contact printing". In: *Lab Chip* (2014), pages. DOI: 10.1039/C4LC00050A. URL: http://dx.doi.org/10.1039/C4LC00050A.

[36] Charlie Gosse and Vincent Croquette. "Magnetic Tweezers: Micromanipulation and Force Measurement at the Molecular Level". In: *Biophysical Journal* 82.6 (2002), pp. 3314–3329. ISSN: 0006-3495. DOI: 10.1016/S0006-3495(02)75672-5.

[37] Tadashi Matsunaga et al. "High-Efficiency Single-Cell Entrapment and Fluorescence in Situ Hybridization Analysis Using a Poly(dimethylsiloxane) Microfluidic Device Integrated with a Black Poly(ethylene terephthalate) Micromesh". In: *Analytical Chemistry* 80.13 (2008), pp. 5139–5145. DOI: 10.1021/ac800352j.

[38] Vincent J. Sieben et al. "An integrated microfluidic chip for chromosome enumeration using fluorescence in situ hybridization". In: *Lab Chip* 8 (12 2008), pp. 2151–2156. DOI: 10.1039/B812443D.

[39] Indumathi Vedarethinam et al. "Metaphase FISH on a Chip: Miniaturized Microfluidic Device for Fluorescence in situ Hybridization". In: *Sensors* 10.11 (2010), pp. 9831–9846. DOI: 10.3390/s101109831.

[40] Gerard H. Markx and Christopher L. Davey. "The dielectric properties of biological cells at radiofrequencies: applications in biotechnology". In: *Enzyme and Microbial Technology* 25.3–5 (1999), pp. 161–171. ISSN: 0141-0229. DOI: http://dx.doi.org/10.1016/S0141-0229(99)00008-3.

[41] Tao Sun and Hywel Morgan. "Single-cell microfluidic impedance cytometry: a review". In: *Microfluidics and Nanofluidics* 8.4 (2010), pp. 423–443. ISSN: 1613-4982. DOI: 10.1007/s10404-010-0580-9.

[42] Camille Denoeud. *On-chip trapping of spermatozoa for individual analysis*. 31 2012.

[43] Inge van de Ven. *FISH staining of spermatozoa*. May 2013.

[44] C.T. Wittwer, K.M. Ririe, and R.P. Rasmussen. *Annealing Curve Analysis In PCR*. Oct. 2012. URL: US%20Patent%20App.%2013/465,364.

[45] William E. Evenson et al. "1H and 13C NMR Assignments for the Cyanine Dyes SYBR Safe and Thiazole Orange". In: *The Journal of Organic Chemistry* 77.23 (2012), pp. 10967–10971. DOI: 10.1021/jo3021659.

[46] Chemical Book. *Propidium iodide: Basic information*. 2008.

[47] Life Technologies. *LIVE/DEAD Sperm Viability Kit (L-7011)*. 2001.

[48] ID Labs. *Porcine IDetect Chromosome Paint Probes FISH Protocol*. 2011.

[49] Chemical Book. *DAPI: Basic information*. 2008. URL: http://www.chemicalbook.com/ProductChemicalPropertiesCB21373008_EN.htm.

[50] Protein Data Bank. *The structure of DAPI bound to DNA*. 2014. URL: http://www.rcsb.org/pdb/explore/jmol.do?structureId=1D30&opt=3.

[51] *DAPI Spectra*. 2014. URL: http://www.uni-leipzig.de/~strotm/equipment/spectra/spectra_dapi.html.

Appendix A

Protocols

A.1 Viability staining

1. Dilute the boar semen sample in sperm medium 20x.
2. Prepare a 50x dilution of the SYBR 14 stock solution in buffer.
3. Add 5 µl of the diluted SYBR 14 and 5 µl PI stock solution to 190 µl of the diluted boar semen.
4. Incubate for 10 minutes.
5. Observe the item through a fluorescence microscope.

A.2 FISH Staining

I. Sample processing and cell fixation

1. For the sample preparation, mix 0.5ml sperm sample and 9ml sperm medium in a 10ml centrifuge tube.
2. Centrifuge the tube for 5 minutes at 1200 rpm.
3. Remove the supernatant with a Pasteur pipette.
4. Add a pre-heated (37°C) hypotonic solution (KCl 0.075M) drop by drop to the pellet to obtain a final volume of 10ml. Add slowly to prevent bursting of the cells, tail (sometimes) falls of at this stage.
5. Place the tube in a 37°C water bath for 30 minutes.
6. Again centrifuge the tube for 5 minutes at 1200 rpm.
7. Carefully discard the supernatant by decantation.
8. Add the Carnoy's fixative (methanol:acetic acid, 3:1) at 4°C drop by drop to the pellet to obtain a final volume of 8ml.
9. Then centrifuge the tube again for 5 minutes at 1200 rpm.

10. Discard the supernatant by decantation.
11. Mix the pellet with 1ml Carnoy's fixate.
12. The fixated mixture can now be stored at -20°C and used for every new experiment on cleaned glass slides (previously stored in methanol at -20 °C).
13. Air-dry the slides and pipette 10 µl of the mixture onto the slide.
14. Leave the prepared slides to dry for 10 minutes. (Do not leave for too long, then the mebranes will harden too much)

II. Decondensation

1. Place the slides in two consecutive coplin jars with 2xSSC solution for 3 minutes each.
2. Place the slides were placed through a series coplin jars with 70%, 85% and 100% ethanol for 2 minutes each.
3. Let the slides dry at room temperature.
4. Transfer the slides to a pre-heated (37°C) freshly prepared dithiothreitol (DTT) solution (1,4-dithiothreitol 5mM, 1% Triton X-100 (detergent), 2-Amino-2-(hydroxymethyl)-1,3-propanediol 50mM) for 15 minutes in a 37°C water bath.
5. Immediately repeat steps 1. to 3.

III. Hybridization

1. Prepare the probe mixture by mixing 2.5 µl IDetect Porcine Probe with 2.5 µl hybridization buffer for each slide.
2. Pipette 5 µl probe mixture on every slide.
3. Cover the probe with a coverslip and seal it with cement or by placing it in a specialised holder to prevent evaporation.
4. Place the slide in a 74°C water bath for 3 minutes to denature the DNA.
5. Place the slides in a 37°C stove and leave to hybridize overnight.

IV. Post-hybridization washes

1. Do the next steps per slide, one at a time
2. Remove the cement or holder.
3. Place the slide in a coplin jar with a 2X solution (2XSSC and 0.1% Tween-20) to remove the coverslip.
4. Transfer the slide to a coplin jar with pre-heated (74°C) 0.4X solution (0.4XSSC and 0.3% Tween-20) and place it in a 74°C water bath for 2 minutes.

5. Transfer the slide to the coplin jar with the 2X solution for 1 minute.
6. Rinse the slide briefly in Milli-Q and air-dry them.
7. If desired, counterstain the sample with 5 µl DAPI/Vectashield. Otherwise, use ony Vectashield.
8. Cover the slide with a cover slip and seal it with cement.
9. The slide can now be stored at -20°C or 4°C.

V. Visualization

The slides can visualized with a fluorescence microscope at the wavelengths 402nm, 488nm and 561nm.

A.3 PDMS chip fabrication

1. Weigh 30 g polymer base and 3,0 g cross linker (light sensitive) in a 50 ml tube; the mass ratio needs to be 10 to 1.
2. Mix these components together for 1 to 3 minutes at high speed to obtain a homogeneous mixture.
3. Degas the mixture in a vacuum bell for at least 45 minutes to remove air bubbles from the viscous liquid.
4. Put the wafer in an aluminumfoil covered glass petri dish to form a container for the liquid mixture.
5. Pour the degassed mixture onto the wafer and degas it again for 30 minutes if air bubbles are present.
6. Let the PDMS cure for at least 3 hours in an oven at 60 °C to ensure the cross-linking of the polymer.
7. Pull the cured PDMS from the wafer and cover the textured polymer surface with scotch tape to keep it clean.
8. Remove part of the tape and cut separate chips from the PDMS plate with a razorblade.
9. Puncture holes in the chip with a hollow needle of the desired width to form in- and outlets.
10. Cover the chips again with SCOTCH tape.
11. Clean the surface of a glass slide on which the PDMS chips will be sealed with scotch tape.
12. To facilitate the sealing of the PDMS on glass, treat the textured surfaces of the PDMS and the microscope slide with oxygen plasma in a plasma cleaner for 45 seconds at 400 mTorr. The oxygen plasma oxidizes the polymer surface to silanol (Si–OH).
13. Put the treated PDMS onto the treated glass surface and press carefully to seal properly.

14. Place the slides in an oven at 60°C for 30 minutes. This ensures the formation of covalent Si–O-Si bonds, permanently sealing the surfaces together.

15. Store the microfluidic PDMS-chips in demineralized water to preserve hydrophilicity.

A.4 FISH Staining on Chip

(The flow rates mentioned below for trapping may differ slightly per chip)

I. Sample processing and cell fixation

1. For the sample preparation, mix 50 µl sperm sample and 950 µl sperm medium in a 10ml centrifuge tube, vortex the mixture before use.

2. Pipette 40 µl sperm dilute into well A and B of the chip.

3. Flow the dilutent through the channel with 0.5 µl/min for 5 minutes.

4. Adjust the flow to 0.05 µl/min for the channel connected to well A and to 1 µl/min for the other channel.

5. Dry the wells with a fibreless tissue.

6. Pipette 40 µl sample into well A and pipette 40 µl sperm medium into well B.

7. Wait until a sufficient amount of cells are trapped (flow rates might have to be adjusted for different chips).

8. Dry the wells with a fibreless tissue.

9. Pipette 40 µl hypotonic solution (KCl 0.075M) into well A and B.

10. Heat the sample to 37°C with the use of a hot plate.

11. Adjust the flow to a pulsating flow with 0.05 µl/min for 1 minute and no flow for one minute for both channels for 30 minutes.

12. Turn off the hot plate.

13. Dry the wells with a fibreless tissue.

14. Pipette 40 µl Carnoy's fixative (methanol:acetic acid, 3:1) into well A and B.

15. Keep the pulsating flow for 10 minutes.

II. Decondensation

1. Adjust the flow to 0.05 µl/min.

2. Dry the wells with a fibreless tissue.

3. Pipette 40 µl 2xSSC solution into the wells.

4. Flow 2xSSC solution through the channels for 6 minutes.

5. Dry the wells with a fibreless tissue.
6. Pipette 40 µl 70% ethanol into the wells and flow it through for 2 minutes.
7. Dry the wells with a fibreless tissue.
8. Pipette 40 µl 85% ethanol into the wells and flow it through for 2 minutes.
9. Dry the wells with a fibreless tissue.
10. Pipette 40 µl 100% ethanol into the wells and flow it through for 2 minutes.
11. Dry the wells with a fibreless tissue.
12. Pipette 40 µl freshly prepared dithiothreitol (DTT) solution (1,4-dithiothreitol 5mM, 1% Triton X-100 (detergent), 2-Amino-2-(hydroxymethyl)-1,3-propanediol 50mM) into both wells .
13. Heat the sample to 37°C with the use of a hot plate.
14. Adjust the flow to a pulsating flow (0.05 µl/min for 1 minute and no flow for one minute) for 20 minutes.
15. Immediately repeat steps 1. to 9.

III. Hybridization

1. Prepare the probe mixture by mixing 0.5 µl IDetect Porcine Probe with 0.5 µl hybridization buffer.
2. Dry the wells with a fibreless tissue.
3. Pipette 40 µl hybridization buffer into the wells.
4. Dry well A with a fibreless tissue.
5. Pipette 1 µl probe mixture into well A.
6. Adjust the flow to 0.25 µl/min.
7. Flow the probe mixture through until the channel is completely filled, then stop the flow.
8. Seal the wells with parafilm .
9. Place the chip on a 74°C hot plate for 3 minutes to denature the DNA.
10. Place the chip (including tubing) in a 37°C stove and leave to hybridize overnight.

IV. Post-hybridization washes

1. Place the chip (including tubing) back in the set-up
2. Remove the parafilm.
3. Dry the wells with a fibreless tissue.
4. Pipette 40 µl 0.4X solution (0.4XSSC and 0.3% Tween-20) into the wells.

5. Adjust the flow to 0.25 µl/min for 1 minute.
6. Stop the flow for 3 minutes, of those 3 minutes, place the chip on a 74°C hot plate for 2 minutes and 30 seconds.
7. Adjust the flow to 0.1 µl/min.
8. Dry the wells with a fibreless tissue.
9. Pipette 40 µl 2X solution (2XSSC and 0.1% Tween-20) into the wells.
10. Flow the 2X solution through the channels for 1 minute.
11. Dry the wells with a fibreless tissue.
12. Pipette 40 µl Milli-Q into the wells.
13. Flow the Milli-Q through the channels for 1 minute.
14. Dry the wells with a fibreless tissue.
15. Pipette 40 µl Vectashield (optionally with DAPI) into the wells.
16. Flow the Vectashield through the channels for 1 minute.
17. Cover the in- and outlets with a cover slip.
18. The slide can now be stored at 4°C.

V. Visualization The chip can be visualized with a flourescence microscope at the wavelengths 402nm, 488nm and 561nm.

Appendix B

Used fluorescent dyes and probes

B.1 Viability staining

For viability staining the dyes propidium iodide and SYBR 14 were used. The SYBR 14 is able to permeate the cell membrane, so it will bind to the DNA in every cell, while propidium iodide will only stain the dead cells, whose cell membranes are not intact.

SYBR 14 binds to the DNA strand by situating itself between two base pairs, which is called intercalating. The structure of this compound is kept secret by the company that made it, but will probably look similar to the dyes SYBR Green I and SYBR Safe, whose structures are known.

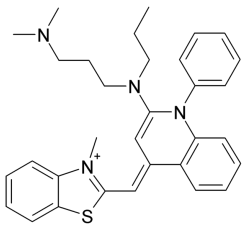

Figure B.1: SYBR Green I [44]

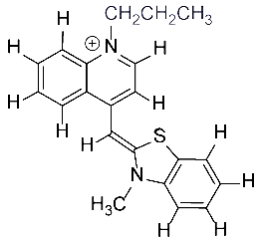

Figure B.2: SYBR Safe [45]

Propidium iodide (PI) is an intercalating dye that is not able to permeate the cell membrane. Propidium iodide is very toxic, so the exposure time of the cells is crucial. It has a larger affinity for binding to the DNA than SYBR 14, so when a cell dies, the PI will expel the SYBR 14.

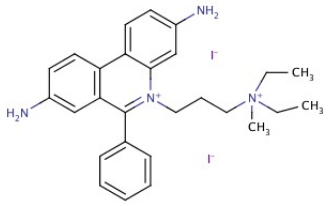

Figure B.3: Propidium Iodide [46]

Both SYBR 14 dye and propidium iodide can be excited with visible-wavelength light. When bound to DNA, the fluorescence emission maxima of these dyes are 516 nm (green) and 617 nm (red) respectively.

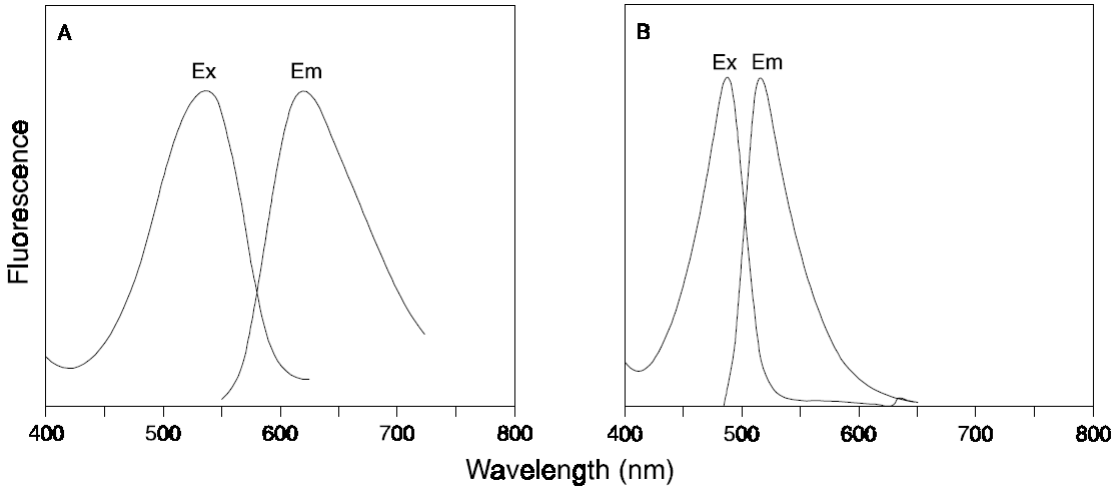

Figure B.4: Exitation and emission spectra for A) Propidium iodide and B) SYBR 14 [47]

B.2 FISH staining

For the FISH staining in this work the red and green porcine probes have been used, which have an emission maximum at 573 nm and 521 nm respectively. The red probe binds to the Y chrmosome, while the green probe binds to the X chromosome.

IDetect™ FISH probes in 5 colours from ID Labs™

Colour	Fluorochrome	Ex. (nm)	Em. (nm)
Aqua	IDYE™ 415	418±15	467±10
Green	IDYE™ 495	493±10	521±10
Red	IDYE™ 556	548±15	573±20
Orange	IDYE™ 616	611±10	631±15
Far-Red	IDYE™ 647	653±10	672±10

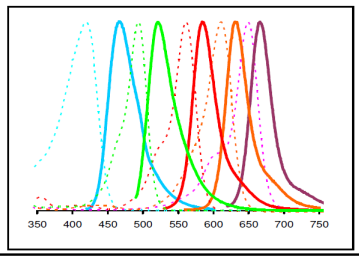

Figure B.5: Exitation and emission spectra for porcine IDetect probes [48]

Another dye that is used is DAPI, which is able to permeate the membrane. It is possible to dye the sample after the FISH staining with a DAPI solution. DAPI binds to the minor groove of the DNA helix, and the staining can thus be done after the hybridization step. This is a control step in the protocol to find the cells. However, adding DAPI to the sample might reduce the visibility of the green X probe, as their excitation wavelengths overlap slightly. DAPI is excited at 360 nm and emits at 460 nm (blue) when bound to DNA.

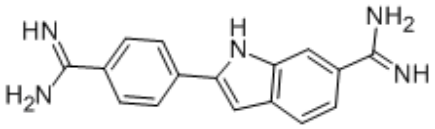

Figure B.6: DAPI molecular structure [49]

Figure B.7: DAPI-DNA complex [50]

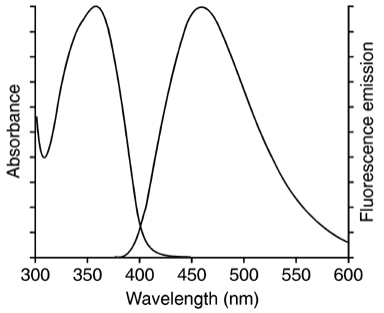

Figure B.8: Exitation and emission spectra for DAPI [51]

Appendix C

Alignment tool

A costum made alignment tool was used for the alignment of the PDMS chip and the glass chip with electrodes. It could be placed under a stereomicroscope. The device made use of four needles that were inserted in the chip and allowed for three degrees of freedom in the alignment. The chip was first placed on a plateau where it rested on its four corner. The device was then lowered to insert the needles, after which it was lifted and could be aligned at a distance of only a few micrometer.

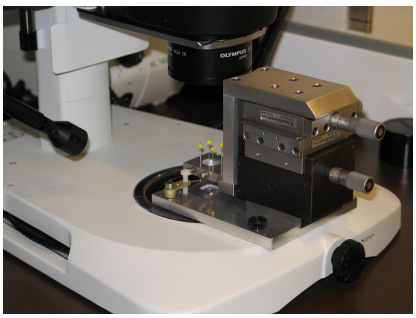

(a) Alignment tool with the stereomicroscope.

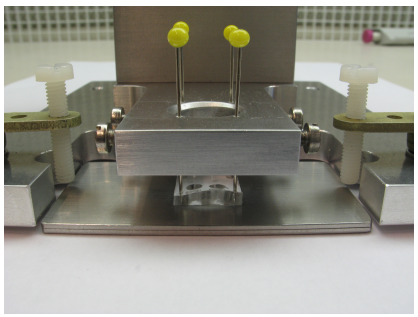

(b) Needles are inserted into the PDMS chip.

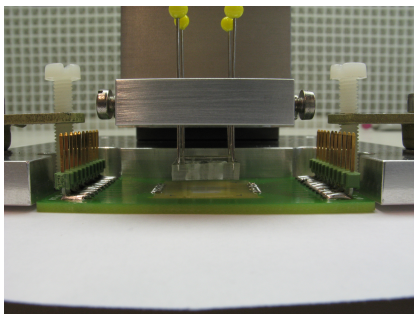

(c) Alignment of the chip.

Figure C.1